

HEALY, JAMES PATRICK, Ph.D. A Thermodynamic Model of RXR Self-Association and Ligand Binding. (2014)  
Directed by Dr. Vincent Henrich. 74 pp.

This study looked at the thermodynamics of ligand binding to the Retinoid X Receptor (RXR) and the formation of the RXR auto-repressive tetramer. Often called the “Master Coordinator” RXR is a required partner for activation of class II nuclear receptors. The first part used isothermal titration calorimetry (ITC) and site-directed mutagenesis to isolate and characterize the binding of a set of chemically diverse ligands to the RXR ligand binding domain.

It was found that a molecule’s shape and flexibility play a crucial role in determining a ligand’s preference for the active or inactive form of RXR. These data showed that many RXR ligands appear to bind in a much stronger manner than was previously suggested by gene activation studies performed in cell culture. Furthermore it was shown that the shape of the potential ligand, whether it is bent or straight, as well as the amount of available molecular flexibility determine which RXR form a ligand will preferentially bind to

The second part of the study used ITC and native-PAGE electrophoresis to model the formation and dissociation of the RXR tetramer. The initial model under consideration was a three stage model of monomer – dimer-tetramer equilibrium. However, non-linear curve fitting analysis of the proposed model to experimental data showed that RXR tetramer dissociation is much more exothermic than the model predicted. This led to a proposed more complex model for the tetramer formation which addresses the larger than expect energy release.

A THERMODYNAMIC MODEL OF RXR SELF-ASSOCIATION AND LIGAND BINDING

by

James Patrick Healy

A Dissertation Submitted to  
the Faculty of The Graduate School at  
The University of North Carolina at Greensboro  
in Partial Fulfillment  
of the Requirements for the Degree  
Doctor of Philosophy

Greensboro  
2014

Approved by

---

Committee Co-Chair

---

Committee Co-Chair

APPROVAL PAGE

This dissertation written by James Patrick Healy has been approved by the following committee of the Faculty of The Graduate School at The University of North Carolina at Greensboro.

Committee Co-Chair \_\_\_\_\_  
\_\_\_\_\_

Committee Members \_\_\_\_\_  
\_\_\_\_\_

\_\_\_\_\_  
Date of Acceptance by Committee

\_\_\_\_\_  
Date of Final Oral Examination

## TABLE OF CONTENTS

	Page
CHAPTER	
I. SPECIFIC AIMS AND HYPOTHESES.....	1
Specific Aim 1 .....	1
Specific Aim 2 .....	2
II. BACKGROUND AND SIGNIFICANCE .....	4
Background.....	4
Tetramer Structure.....	9
Homodimer Structure.....	10
RXR Ligand Binding Pocket.....	10
III. RESEARCH DESIGN AND METHODOLOGY.....	16
Expression and Purification of Recombinant Protein .....	16
Site Directed Mutagenesis .....	17
Native PAGE and SDS-PAGE Electrophoresis and Western Blot Analysis.....	17
Isothermal Titration Calorimetry .....	18
Ligand Binding Analysis.....	24
Modeling the RXR-LBD Tetramer Formation .....	29
IV. DISCUSSION AND CONCLUSIONS.....	37
Ligand Binding Study .....	37
Tetramer Dissociation Modeling.....	39
Future Directions.....	43
WORKS CITED .....	44
APPENDIX A. DERIVATIONS.....	50
APPENDIX B. POOLED STANDARD DEVIATION .....	54
APPENDIX C. ORIGIN FITTING PROGRAM.....	55

APPENDIX D. NATIVE PAGE DATA .....	60
APPENDIX E. ITC THERMOGRAMS.....	63

## CHAPTER I

### SPECIFIC AIMS AND HYPOTHESES

The nuclear hormone receptor (NR) family of proteins plays critical roles in a variety of cellular signaling pathways within the human body<sup>1</sup>. Through their binding of a “drug-like” ligand molecule, NRs regulate the expression of a wide number of gene networks in the cell<sup>2</sup>. Among NRs, the Retinoid X Receptor (RXR) is particularly important. Often referred to as the “Master Coordinator”, RXR is a required heterodimer for an entire class of NRs<sup>3</sup>

The ligand binding domain (LBD) of RXR has a mechanism of self-regulation and activation through the formation of *apo*-tetramers that dissociate upon ligand binding and form activated homo- or heterodimers<sup>4</sup>. This pathway is not completely understood, particularly because there are few direct biophysical measurements of the kinetic and thermodynamic parameters of these pathways. This study makes use of isothermal titration calorimetry (ITC) in conjunction with normal RXR LBD and mutant RXR LBD versions produced by site directed mutagenesis to isolate the events associated with RXR multimerization and obtain direct biophysical measurements of this mechanism.

**Specific Aim 1:** To obtain specific and direct biophysical measurements of the interactions of different ligands with RXR and observe the ligand effects on the relative amounts of different RXR complexes.

The current scientific literature contains a wealth of data on RXR-ligand interactions from in-vitro and cell signaling assays.<sup>5 6 7</sup> Since ITC directly measures the energies of interaction between two molecular species, information on interactions that

cannot be studied with in-cell assays such as ligand binding can be obtained. ITC was used to characterize the interactions of RXR with different known ligands including the fatty acids, docosahexanoic acid (DHA) and phytanic acid which have been hypothesized to be endogenous ligands for RXR<sup>8</sup>. Also tested was 9-*cis*-retinoic acid (9*cis*RA), the classical RXR ligand<sup>9</sup> and Dantron, an RXR antagonist which stabilizes the inactive tetramer of RXR<sup>10</sup>.

Fatty acids such as DHA and phytanic acid, should show the ability to interact with RXR in both tetrameric and dimeric forms. This expectation is based upon evidence that the RXR ligand binding pocket adopts a linear “I-shaped” conformation while in its inactive state and undergoes a conformational shift to a bent “L-shaped” conformation in its active ligand bound shape<sup>11</sup>. Both DHA and phytanic acid are flexible fatty acid molecules which should be able to match either conformation of RXR. This is unlike 9*cis*RA and Dantron, which are rigid molecules and are predicted to show strong interactions with RXR in only one form.

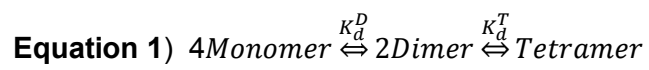
Furthermore with data from several different ligands, structural features which predispose a molecule to dissociate or stabilize different RXR multimers can be begin to be identified. This could allow for development of potential therapeutics which can interact with and interrupt the regulation of RXR complex formation by ligands, whether natural or artificial.

**Specific Aim 2:** To develop a thermodynamic model of RXR complex formation and dissociation- using Isothermal Titration Calorimetry (ITC).

By using thermodynamic data obtained from ITC, a proposed model of RXR multimer formation and dissociation will be explored. In this study the effects of different mutant RXR proteins will be measured with ITC and the energies associated with the

formation of each species will be measured. Site directed mutations of RXR will be used to test protein-protein interactions of RXR mutants that predictably disrupt the normal formation of monomers, dimers, and tetramers.

It was hypothesized that the likely equilibrium system to represent the distribution and formation of each RXR-LBD multimeric states could be written as below





## CHAPTER II

### BACKGROUND AND SIGNIFICANCE

**Background:** Nuclear Receptors (NRs) are a family of transcription factors that reside in the cytoplasm and nucleus of cells<sup>1</sup>. NRs are defined by the presence of a DNA binding domain that contains two cysteine-cysteine zinc fingers separated by a linker region. This domain is responsible for direct interaction with specific DNA sequences. NRs regulate a variety of developmental, homeostatic, and metabolic functions at the cellular level<sup>12</sup>. Typically a NR acts by binding a small lipophilic molecule such as a steroid, vitamin, fatty acid or other dietary metabolite<sup>13</sup>.

With the widespread interactions of the nuclear receptor superfamily with almost all aspects of human physiology, the role of these receptors in many human diseases, and their importance as therapeutic targets for pharmaceuticals, it is obvious that the understanding of them has implications, not only for human biology but also for the understanding and development of new drug treatments<sup>2</sup>.

In general, ligand binding, causes the receptor's conformation to change from an inactive to an active conformation. This activation often results in the homo- or heterodimerization of the NR and binding of the now-activated NR to specific sequences of DNA in the genome known as response elements (REs)<sup>14</sup>. Once bound to its specific RE the receptor begins recruitment of other transcription or repression factors, thereby causing the up-regulation or down-regulation of a target gene's expression<sup>15</sup>. These activating ligands are often low molecular weight, hydrophobic molecules. These "drug-like" qualities of the NR's ligand molecules along with their far-reaching influence into all

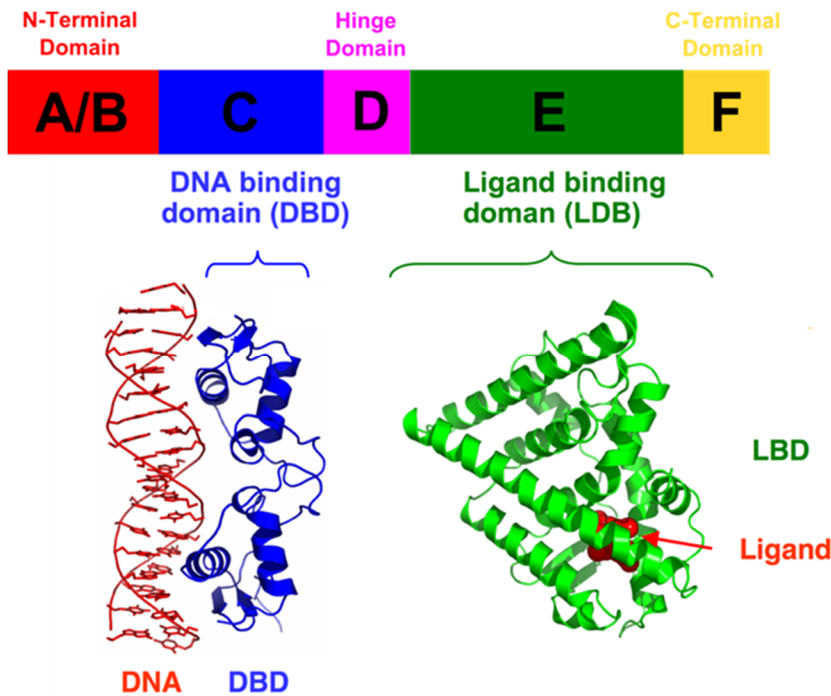
parts of human physiology have made them attractive targets for pharmaceutical development<sup>16</sup>.

The NR family is roughly divided into four classes based on their mechanisms of activation and binding to response elements (REs)<sup>1</sup>. REs are short sequences of DNA found within the promoter region of a gene which have the ability to bind specific transcription factors in order to regulate transcription of the associated gene. Type I NR's (Steroid Receptors) typically bind as ligand bound homodimers to hormone response elements (HREs) consisting of two half-sites that are separated by a variable length of DNA. The second half-site contains a sequence inverted from the first site (an inverted repeat). Type II NR's (RXR Heterodimers) function as heterodimers with RXR as the dimerization partner and function in a ligand dependent manner. These dimeric complexes usually bind to direct repeat response elements in contrast to type I NR's. In the absence of ligand, type II nuclear receptors are often found in complex with corepressor proteins. Binding of ligand to the NR causes dissociation of the co-repressor and recruitment of coactivator proteins. Type III (Dimeric Orphan Receptors) NRs bind to DNA as homodimers, similar to type I receptors. However, type III NR's bind to direct repeat HREs unlike type I NRs which bind to inverted repeat HREs. Like other NR classes Type IV NR's (Monomeric or Tethered Receptors) can bind either as monomers or dimers. Unlike other NRs however, only a single DNA binding domain (DBD) of the receptor binds to a single half site of an HRE regardless of any dimerization the receptor may undergo<sup>17</sup>.

The sub-family of nuclear receptors known as class II or RXR heterodimer receptors contains the Vitamin D Receptor (VDR), Peroxisome Proliferators-Activated Receptors (PPARs), Farnesoid X Receptor (FXR) and the Thyroid Hormone Receptor

(TR) among others. Members of this subfamily require the Retinoic X Receptor (RXR) as a dimeric partner to regulate transcriptional activity. This central regulatory position has led to RXR being described as the “master coordinator”<sup>3</sup>.

RXR holds a unique position in the NR family for more than its role as a “Master Coordinator.” In addition to its heterodimeric capability, it is active as a homodimer and it adopts a scheme of self-inactivation/regulation not found in other members of the family. Although the receptor only contains a single ligand binding site (two in the homodimer), studies have shown that the heterodimeric and homodimeric transcriptional activity may fulfill separate regulatory functions<sup>6</sup>. Across all four classes, NRs share a modular construction consisting of several shared domains (see Figure 1). The N-terminal or A/B domain is highly variable in sequence among the nuclear receptors. The C domain is a highly conserved domain containing the DNA binding domain (DBD) of the NR. The DBD consists of two zinc fingers responsible for binding to the hormone response elements (HREs) in order to modulate expression of their associated genes. The cysteine-cysteine zinc fingers within the DBD are the defining structural domain for most members of the nuclear receptor superfamily. The D domain is a flexible “hinge” domain which connects the DBD with the LBD. Though the D domain’s function is not completely understood some have postulated a role in regulation of DNA binding and subcellular distribution in some NRs.



**Figure 1. Arrangement of a Typical Nuclear Receptor Domain's**

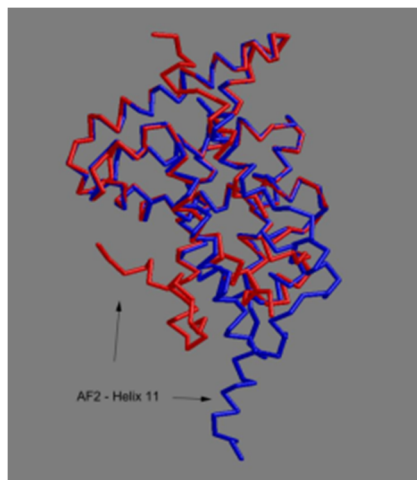
This figure shows the typical layout of the different domains of a nuclear receptor with important features identified within those domains. <sup>16,15</sup>

The E region is the ligand binding domain (LBD). While the LBD generally shows moderate amino acid sequence conservation, its secondary structure is highly conserved among different NRs. The common structural motif of the LBD is what is generally referenced to as an alpha helical sandwich. The LBD also generally contains the dimerization interface of the receptor.

NRs contain two separate activation domains for the recruitment of cofactors and repressor proteins that regulate gene expression. These are called activation function 1 (AF-1) and activation function two (AF-2)<sup>16</sup>. The AF-2 requires the presence of a bound ligand for activation and transcriptional activity. In contrast the AF-1 domain, located in the A/B domain, shows basal transcriptional activation, though it is normally very weak,

but sometimes synergizes with AF-2 to produce stronger up-regulation of gene expression upon ligand binding.

Several crystal structures exist in the literature of RXR, both full length RXR and of the RXR-LBD only. A few are of particular interest in terms of this study. Bourguet *et al.* published a structure of the RXR-LBD (1LBD) which highlights the movement of the AF-2 helix upon ligand binding (See figure 2)<sup>18</sup>. Published crystal structures reveal that the LBD contains 13  $\alpha$ -helices and two  $\beta$ -strands folded into a helical “sandwich” which form a hydrophobic ligand-binding pocket.



**Figure 2. Superimposition of crystal structures of apo-RXR-LBD (blue) and ligand bound RXR-LBD (red)** <sup>24</sup>

In the apo-RXR structure, the AF-2 helix extends downward from the  $\alpha$ -helical “sandwich” and provides an entry point for the ligand. Agonist-bound structures have the AF-2 helix packed against the body of the receptor, forming an essential part of the charge clamp for recruitment of coactivator proteins<sup>18</sup>.

Two other structures of importance to this study are 1MV9<sup>11</sup> and 1G5Y<sup>18</sup> which show RXR bound to DHA and 9cisRA respectively. These structures will be discussed

later in more detail later but are important in the context of this study as they show the conformational difference in the ligand binding pocket in the tetrameric and dimeric forms.

**Tetramer Structure:** In the absence of ligand, RXR exists as a homotetramer<sup>4</sup>. These tetramers retain DNA binding capacity but lack the ability to recruit transcriptional cofactors. Since RXR monomers retain their homodimerization ability regardless of ligand binding, previous study has shown that this tetrameric form performs an additional autorepressive function beyond binding to and blocking expression of RXR controlled response elements. The sequestering of RXR monomers into tetramers apparently limits availability of the RXR monomer for heterodimerization<sup>19</sup>.

The RXR tetramer is a compact, disc-shaped tetramer formed of four RXR LBD monomers. H10 of each monomer forms the main part of each's dimer interface. Each monomer has three main areas which make up the tetramer interface: the H3/H3 interface, the H11/H11 interface, and the interface between the H12 and coactivator binding site. The main portion of the tetramer interface is formed by the H11 helix of each monomer in the upper dimer being packed against the corresponding H11 helix in the lower dimer. The AF-2 helix follows H11, protruding outward from each LBD into the coactivator binding site of the corresponding monomer in the lower dimer. The RXR tetramer structure is an autorepressed complex, assembled from two symmetric dimers that cross-repress each other through the extended AF-2 helices. The H3/H3 interface is made up of the amino-terminal end of H3 from the upper dimer monomer and the amino-terminal end of H3 of the adjacent monomer in the lower dimer<sup>11</sup>.

**Homodimer Structure:** The RXR homodimer was described by Gampeet *al* as “Butterfly shaped, with two symmetric monomers rotated 180° relative to each other around the twofold axis<sup>11</sup>.” Residues from H7, H9, as well as the loop connecting H8 and H9 contribute most of the charged interactions including the formation of complementary hydrogen bonds. The majority of the dimer interface is comprised of non-polar interactions resulting from a paired-coil structure of H10. Interestingly, several polar interactions in the PPAR/RXR heterodimer are missing in the RXR homodimer interface<sup>20</sup>. Some combination of these may also be missing in other RXR heterodimers although these have not been confirmed<sup>21</sup>. If so these could play in role in the observed preference for certain heterodimer formation versus others or homodimer formation.

**RXR Ligand Binding Pocket:** When discussing the ligand binding pocket of RXR s an orientation where the “top” of the monomer in question is defined as the portion exposed to solvent and directly opposite the AF-2 helix will be used. With this orientation the ligand binding pocket of RXR can be described as follows: H5 forms the top with H11 on the bottom, H3 on the right with H7 and H10 on the left and the  $\beta$ -hairpin on the back. The pocket is accessible to the solvent on the left side between H11 and H3<sup>22</sup>.

Ligand binding to the RXR LBD, induces a change in the conformation of the AF-2 helix. This releases corepressor proteins and causes formation of the charge clamp that is capable of recruiting coactivator complexes. These ligand binding events begin a cascade which leads to activation of the target gene and subsequent various physiological changes desired<sup>23</sup>.

Previous crystallographic studies have shown that the RXR ligand binding domain (LBD) adopts two unique conformations. In monomeric or dimeric form the LBD

conformation presents a "L-shaped" ligand binding pocket. This is the form responsible for gene activation via homo- or heterodimerization. The second form is only found within the autorepressive homotetrameric RXR form. In this the conformation the LBD presents a linear "I-shaped" binding pocket<sup>11</sup>. This property offers the possibility of approaching each of these RXR states as separate pharmaceutical targets. Several published studies have already begun to make strides for exploring the distinct pharmaceutical properties of these states.<sup>24 25</sup> Molecular docking simulations have been used to begin designing ligands to activate RXR homo- and heterodimeric functions selectively. RXR self-regulation presents unique opportunities for drug development<sup>26</sup>.

The search for the endogenous RXR ligand has seen much debate and study since the original identification of the receptor. In 1992, Heyman, Mangelsdorf *et al.* undertook a study to answer this question. Mangelsdorf *et al.* hypothesized that since RXR and the retinoic acid receptor (RAR) share similar structural motifs, RXR conceivably binds an isoform of all-*trans*-retinoic acid, the endogenous ligand of RAR. Using from extracts of mouse livers they found via, HPLC and GC/MS that RXR bound 9-*cis*-retinoic acid with a high affinity<sup>9</sup>. At the same time Levin *et al* showed in a study with COS-1 cells expressing RXR that 9-*cis*-RA also bound and activated RXR<sup>27</sup>. Based on these studies, 9-*cis*-retinoic acid was generally accepted as the naturally occurring, endogenous ligand for RXR.

Several further studies in the early 90's ((Yu *et al.*, 1991; Durand *et al.*, 1992; Hallenbeck *et al.*, 1992; Leid *et al.*, 1992; Zhang *et al.*, 1993) showed that RXR is activated in cell culture by 9*cis*RA.<sup>28 29 30 23</sup> Further they showed that once activated RXR can bind to specific DNA response elements and regulate transcription as a



homodimer. The 1991 Yu study first established the existence of RXR $\beta$ , and looked at both RXR $\alpha$  and  $\beta$  as heterodimeric partners for RAR using transfected CV1 cells and monitoring luciferase activity to measure 9cisRA activation of both isoforms for RXR.

Durand *et al.* in a 1992 study used a series of CAT (Chloramphenicol Acetyl Transferase) assays to establish that RXR-RAR heterodimers are responsible for cellular retinoic acid-binding protein II (CRABP II) promoter transactivation. Specifically, they found that the interaction is RXR-RAR specific and not controlled by RAR alone. They identified the pair as working through the DR1 and DR2 direct repeat motifs. Both the Zhang and Hallenbeck studies showed that the Thyroid Hormone Receptor also requires heterodimerization for gene activation.

Later, Ulven *et al.* (2001) investigated the distribution of retinoid along the developing spinal cord of mouse embryos by means of ultrasensitive HPLC/MS. Although RXR was present and the presence of all-*trans*-retinoic acid was easily observable, no 9-cis-retinoic acid could be detected. Urbach and Rando, observed that all-*trans*-retinoic acid shows spontaneous (non-enzymatic) isomerization to 9-cis-retinoic acid<sup>31</sup>. The presence of 1% BSA and SDS, without any source of enzymatic activity, was found to transform all-*trans*-retinoic acid into 9-cis-retinoic acid to levels of approximately 15% isomerization at equilibrium. This finding suggests that the earlier detection of 9-cis-retinoic acid in animal tissues could be the result of spontaneous conversion of the all-*trans*-retinoic acid into the 9-cis-form.

A 2006 genetic study by Chambon showed that for at least one system 9-cis-RA can be definitively excluded as an endogenous RXR ligand<sup>32</sup>. Newborn mouse skin cells produce a characteristic protein called corneodesmosin packaged in small organelles called lamellar granules. The authors found that lamellar granules required the presence

of RAR/RXR heterodimer (with RAR unliganded) and the presence of PPAR/RXR where PPAR is the peroxisome proliferated activated receptor. The RXR in the heterodimer PPAR/RXR is liganded. Furthermore, topical treatments of wild-type newborn mouse skin with 40 nM all-trans-retinoic acid caused the loss of lamellar granules which are seen in RAR knockout cells. The authors proposed two hypotheses. Firstly, two signaling pathways are needed for lamellar granule formation, requiring the nuclear receptor heterodimers RAR /RXR (with the RAR unliganded) and PPAR/RXR(with the RXR bound to a ligand). If 9-cis-retinoic acid were a ligand of the RXR , then the 9-cis-retinoic acid present *in vivo* would also bind to RAR,since RAR is not stereo-selective between 9-cis-retinoic acid or all-trans-retinoic acid. Since granule formation requires unliganded RAR, clearly 9cisRA cannot be an endogenous ligand for RXR in newborn mouse skin cells.

What then is the natural ligand for RXR? Multiple sources have shown RXR to be activated by a variety of long chain fatty acids, primarily phytanic acid and docosahexaenonic acid (DHA).<sup>33-35</sup> Both bind to RXR at low micromolar concentrations (66 $\mu$ M for DHA and 2.3 $\mu$ M for phytanic acid) and are naturally occurring in cells. Also both have been shown to activate pathways in which RXR plays a regulatory role in proteomic studies.<sup>36 37 35 38 39 40</sup> DHA is particularly promising as it has been shown to be a natural RXR ligand in mouse brain tissue<sup>33</sup>.

The current work makes extensive use of isothermal titration calorimetry, or ITC, to study the interactions of RXR monomer both with themselves and ligand molecules. An isothermal titration calorimeter consists of two identical cells made of a thermal conducting and chemically inert material, surrounded by an adiabatic water jacket<sup>41</sup>. Sensitive thermocouple circuits are used to detect temperature differences between the

reference cell (filled with buffer or water) and the sample cell containing the macromolecule. Prior to addition of ligand, a constant power is applied to the reference cell. This directs a feedback circuit, activating a heater located on the sample cell. During the experiment, ligand is titrated into the sample cell in precisely known aliquots, causing heat to be either taken up or released (depending on the interaction under investigation). Measurements then consist of the time-dependent input of power required to keep the reference and sample cells isothermal.

In an exothermic interaction, the temperature in the sample cell increases as the interaction occurs. This causes the feedback power to the sample cell to be decreased in order to maintain an equal temperature between the two cells. In an endothermic interaction, the opposite occurs; the temperature of the sample cell decreases, thus causing more power to be applied via the feedback circuit in order to maintain isothermal conditions

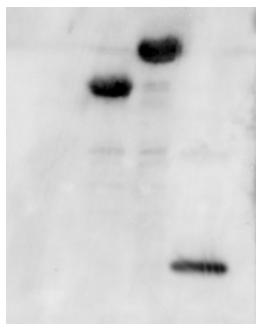
Measurements are plotted as the power needed to maintain the reference and the sample cell at an identical temperature over time. This causes the resulting raw experimental data to consist of a series of spikes of heat flow (measured as changes in power), with every spike corresponding to one injection. By integrating these injection spikes with respect to time, the total heat exchanged per injection can be determined. Thus by looking at these integrated heats as function of the molar ratio, binding affinity ( $K$ ), change in enthalpy ( $\Delta H$ ) and change in entropy ( $\Delta S$ ).

Direct biophysical measurements of ligand interactions with wild-type and mutated forms of the RXR LBD, can give information concerning the extent to which molecular binding events are  $\Delta S$  or  $\Delta H$  driven and how favorable the overall free energy change will be. Eventually, this methodology could allow the rational design of RXR

ligands based on features in addition to strong binding affinity. These measurements can help to provide a framework in which a medicinal chemist can design a molecule to target a specific RXR multimer and then test that molecule, measure ligand/RXR affinity and detect the energy changes brought on by binding ( $\Delta H$ ,  $\Delta S$ ). Furthermore, by careful analysis and control of macromolecule/ligand molar ratios the presence of multiple sequentially binding sites can be detected and cooperativity either positive or negative which might exist between them determined.

CHAPTER III  
RESEARCH DESIGN AND METHODOLOGY

**Expression and Purification of Recombinant Protein:** RXR encoding expression vectors for our study were purchased from DNA 2.0 (Menlo Park, CA). The first is RXR-EF which contains the E and F regions only. The vectors include a promoter for the T7 RNA polymerase and attach a C-terminal 6-histidine (6His) affinity tag. All references to *wt-hRXR $\alpha$*  will refer to this RXR-EF domain clone. The *wt-hRXR $\alpha$*  expression vector was transformed into *E. coli* BL21-DE3 cells. Protein purification was performed by included methodology on His-Trap affinity purification columns.



**Figure 3. Western Blot Analysis of purified protein showing presence of hRXR $\alpha$**

Crude extract and samples of each stage of column elution were saved and checked by SDS-PAGE and presence of hRXA $\alpha$ -LBD was confirmed by Western Blot analysis (Figure 3). Eluted protein was concentrated and elution buffer exchanged with assay buffer using Pierce Concentrators 20k MWCO (Thermo Scientific). Final concentrations were determined by Bradford assay on a NanoDrop 2000

Spectrophotometer. Final protein preparations were used immediately in assays to reduce the possibility of instability of the recombinant LBD.

**Site Directed Mutagenesis:** Site-specific mutants of the RXR-LBD were produced using the Quik-Change II XL Site Directed Mutagenesis kit. The manufacturer's instructions were followed. Primers for site directed mutagenesis (SDM) were designed by hand to give appropriate  $T_m$  and %GC content and then ordered from Integrated DNA Technologies (IDT). For this study, two mutants were produced, F315A and R318A. (See Figure 4) . R318A and F315A have been shown previously to prevent dissociation or formation of the inactive tetramer, respectively.<sup>21 18</sup>

Both mutated plasmids were transformed into bacterial hosts and purified in the same manner as previously described for *wt*-RXR. Purified mutant RXR forms were verified by western blot and non-denaturing PAGE gels to verify the intended effect of the mutations. Both mutations were verified by DNA sequencing of the clone encoding the mutant protein form

**Native PAGE and SDS-PAGE Electrophoresis and Western Blot Analysis:**

Purified proteins samples were analyzed under non-denaturing and denaturing PAGE electrophoresis. For western blotting the initial SDS PAGE was performed on 10% mini TGX gels purchased from Bio-Rad. Following this, the samples were transferred using the Trans Transfer Turbo blot kits from Bio-Rad. Blotted membranes were treated with a RXR specific primary antibody (RXR C-20 rabbit polyclonal, purchased from Santa Cruz Biotech). After this, they were developed with almmunostar AP secondary antibody and substrate kit (BioRad). For Native PAGE, precast Tris-glycine gels were purchased from Bio-Rad with percentages from 7.5% to 10%. Electrophoresis was performed at a pH of

8.0 and at a voltage of 200V and a current never exceeding 45mA. Gels were stained with a Coomassie Blue stain.

**Isothermal Titration Calorimetry:** ITC experiments were performed using a ITC<sub>200</sub> microcalorimeter (Microcal, Inc). Purified RXR LBD was dialyzed against sample buffers to be used in the ITC assays. A concentrated solution of purified and dialyzed RXR-LBD in assay buffer was loaded into the injection syringe while the sample cell was filled with dialyzed assay buffer. If applicable for the experiment, the ligand to be studied was added to the sample cell buffer to the desired concentration. Both sample and reference cells were heated to 28 degrees Celsius. A number of injections were made, with the first being a 0.5 $\mu$ L “throwaway” injection while the final 15 - 20 injections were each between 1.0 and 1.5 $\mu$ L.

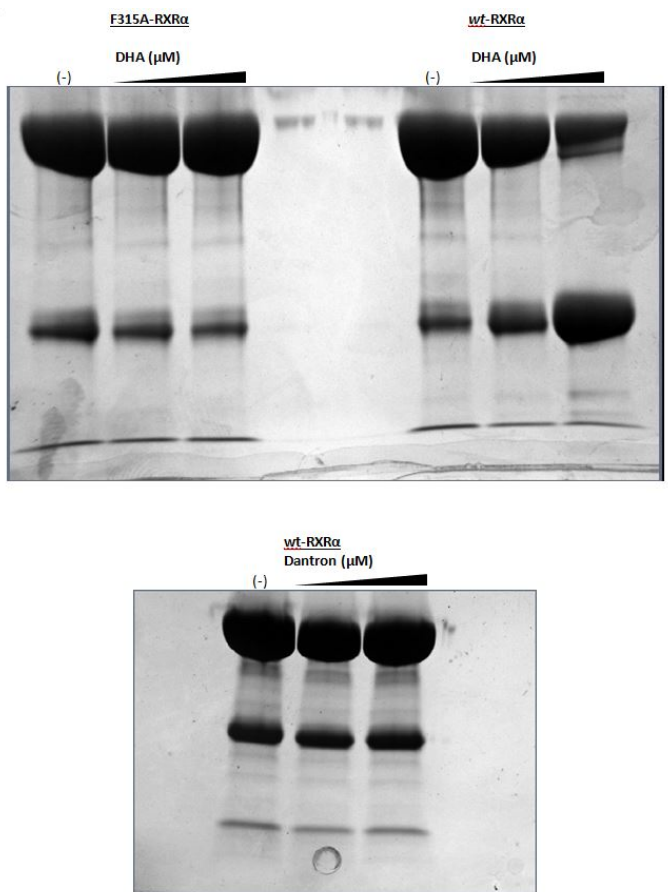
In order to avoid large dilution heats which could mask the heat changes of any interactions, the concentration of organic solvent in the protein solutions must be matched to the concentration in the ligand solution. Since concentrations of more than 1%-2% DMSO will inhibit the activity of our protein, the maximum concentration of ligand was between 50-75 $\mu$ M depending on the ligand.

Two sets of ITC assay's were performed for each RXR-ligand assay. Both involved making injections of concentrated solutions of RXR into the sample cell. In one set the cell contained the ligand to be studied in appropriate buffer and organic solvent needed to ensure solubility. The second was identical to the first except that no ligand was present in the sample cell, though care was taken to ensure that the buffer was identical except for the absence of ligand.

The first goal of the study was to isolate and test the effect of specific point mutations in the RXR $\alpha$ LBD to isolate the different oligomeric states adopted by RXR.

The R318A mutant prevents dissociation of the RXR tetramers upon ligand binding and the, F315A mutant RXR inhibits tetramer formation. Where possible, each mutant was verified using visualization via native PAGE (Figure 4).

In order to verify the multimeric states of RXR Native PAGE electrophoresis was used to monitor these states under non-denaturing conditions.



**Figure 4. Native PAGE Electrophoresis of RXR and RXR mutant forms**

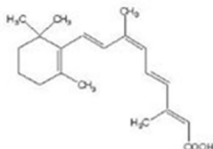
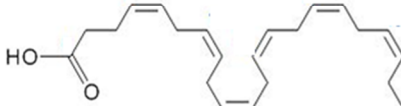

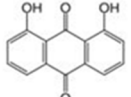
As expected, *wt*-RXR was found to favor the tetrameric state although this equilibrium rapidly shifted to favor the dimeric form with increasing agonist concentration (DHA 1-5μM) (See Fig. 4). The antagonist Danthron did not dissociate the RXR tetramer even at



higher concentrations (5 $\mu$ M) (Figure 4b). A similar effect was seen with the R318A mutant, where the tetramer fails to dissociate with increasing agonist concentration .

The ITC system monitors the changes in power required by the heating units to keep the sample and reference cells isothermal during the injections as a plot of  $\mu$ cal/s vs total time elapsed. Injections are spaced far enough apart that the baseline can return to equilibrium between injections.

By integrating the area under each injection peak with respect to the current macromolecule concentration in the cell, total energy released (in  $\mu$ cal per mole) for each injection can be calculated. This is the plot of integrated heat per mole of injectant vs. molar ratio of macromolecule to ligand as an ITC thermogram.

Ligand	Structure	Action
9- <i>cis</i> -Retinoic Acid(9 <i>cis</i> RA)		Agonist
<u>Docosahexanoic Acid (DHA)</u>		Agonist
<u>Phytanic Acid</u>		Agonist
<u>Danthron</u>		Antagonist

**Figure 5. Ligands under investigation**

Four different ligands of RXR-LBD were tested (See Figure 5). Three are known agonists and one is an antagonist. Two are fatty acids, docosahexanoic acid (DHA) and phytanic acid, both of which have been shown to activate RXR in cell culture assays<sup>32, 29</sup>. Also used is 9-*cis*-Retinoic acid (9cisRA) the classical RXR. Finally, we will use Dantron, an RXR antagonist, shown to bind and stabilize the RXR inactive tetramer<sup>8</sup>. *All-trans*-Retinoic acid was initially investigated as another antagonist for RXR<sup>24</sup> as it shares affinity for the inactive tetramer with Dantron. However, due to the instability of transRA and the readiness with which it will isomerize to 9cisRA in solution it was excluded from this study.

Preliminary studies showed that RXR injections performed in the presence of ligand showed a much greater energy release per mole than the same injections performed without ligand present. This increased energy release in the presence of ligand suggests that interactions between the RXR-LBD and ligand molecules are happening and are strong enough to detect with our methodology.

However the thermogram is a composite of both inactive tetramer dissociation and ligand binding/active dimer formation. In order to isolate the ligand binding events, the thermograms of RXR in the absence and presence of ligand were compared to each other.

The total heat for the injections of RXR-LBD in the absence of a ligand can be expressed as follows,

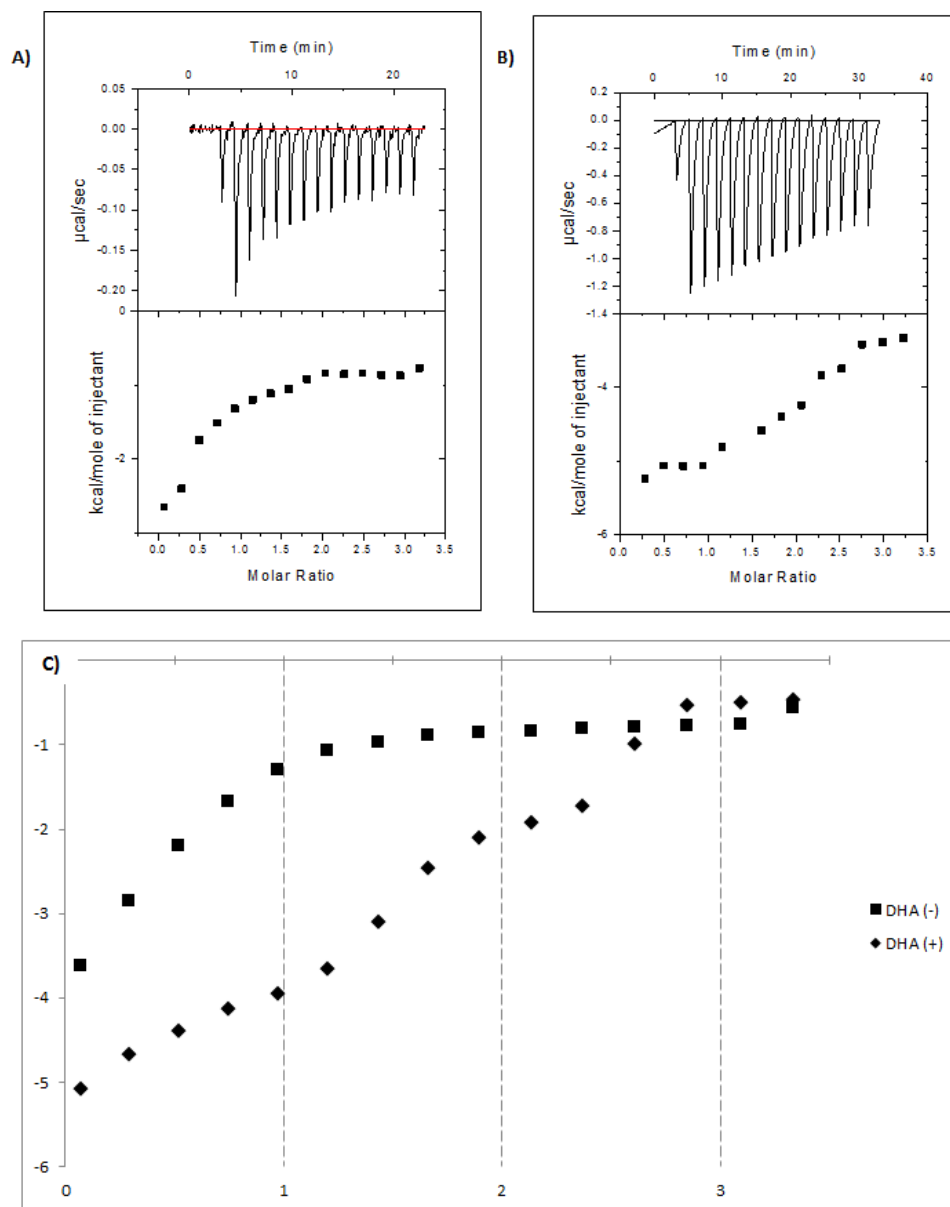
**Equation 2)**  $Q_{tot} = Q_{inactive}$

where the total heat is equal to the heat released from the dissociation of the inactive tetramer.

However, when a ligand for RXR is present the equation for total heat released incorporates multiple terms as there are now two separate events happening with each injection: dissociation of the inactive tetramer to reach equilibrium, binding of ligand, and formation of the active dimer. Therefore the total heat released for each injection can be expressed as follows,

**Equation 3)** 
$$Q_{\text{tot}} = Q_{\text{inactive}} + Q_{\text{bind}}$$

Since heat released is an additive quantity and the ITC experimental protocols are identical between experiments, the thermogram from the ligand negative experiments can be subtracted from those of the ligand positive ones. (Fig 6) This allows for isolation of the energy released unique to the ligand activation events and the ligand binding events.



**Figure 6. Isolation of ligand binding energies**

- A) Raw ITC trace with integrated heats below for titration of *wt*-RXR in the absence of ligand
- B) Raw ITC trace with integrated heats below for titration of *wt*-RXR in the presence of ligand (DHA)
- C) Superimposition of integrated heats of DHA (+) and DHA (-) experiments

**Ligand Binding Analysis:** In measuring binding of potential ligand to RXR-LBD two assumptions were made:

1. Any dissociation of the tetramer due to dilution at each injection happens immediately and before any interaction with the ligand.
2. Each binding site on tetrameric and dimeric RXR-LBD is equally probable.

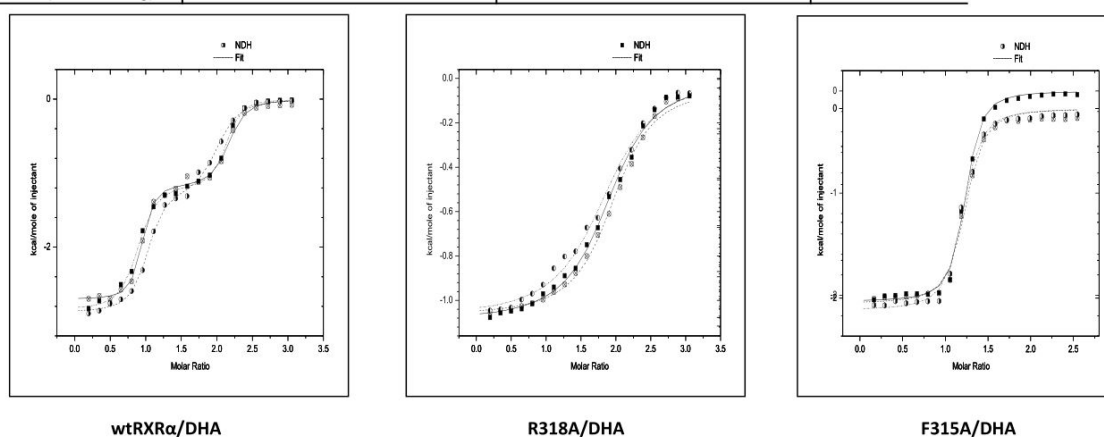
Initial studies showed that titration of *wt*-RXR with known agonists DHA and 9-*cis*-retinoic acid (9*cis*RA) generated a thermogram reflective of a model with two binding sites. This two site binding model became apparent after the heats related to dissociation of tetrameric RXR due to dilution from the ligand binding thermograms were subtracted. A sequential binding model often occurs in biological systems where the binding of a ligand to one site will be influenced by whether or not a ligand is bound to other sites.

In a typical titration with two available sets of sites, the strongest binding of the two sites, whose heat change is H1, will titrate in the early injections while the weaker site, with heat change H2, will titrate in subsequent injections until both are saturated. After this point the heat change will drop to zero.

Since our experiments are performed with ligand injected in the cell, the ligand will be in excess after the initial few injections. This means that both sites will bind ligand with the heat change equaling that of H1 + H2. Once sufficient macromolecule has been added to interact with all of the ligand as the 2-to-1 complex, then further injections of the apo-macromolecule will result in some of the ligand being removed from the weaker site in the 2-to-1 complex so that it can bind to the stronger site on the newly-injected macromolecule. The heat change for this second phase of the titration will then be H1 - H2.

The DHA binding isotherm (See Figure 7) for wt-RXR clearly showed two binding states.

Protein/Ligand	wtRXR $\alpha$ /DHA	R318A/DHA	F315A/DHA
$K_d$ -T (M)	$2.66E-09 \pm 8.1E-09$	$9.84E-06 \pm 2.1E-06$	<b>N/A</b>
$\Delta H$ -T (kcal/mol)	$-3.88 \pm 0.03$	$-1.61 \pm .056$	<b>N/A</b>
$\Delta S$ -T (cal/mol/deg)	25.9	20.8	<b>N/A</b>
$K_d$ -D (M)	$1.12E-06 \pm 8.7E-06$	<b>N/A</b>	$2.16E-07 \pm 3.6E-08$
$\Delta H$ -D (kcal/mol)	$-1.43 \pm 0.044$	<b>N/A</b>	$-2.44 \pm .79$
$\Delta S$ -D (cal/mol/deg)	22.3	<b>N/A</b>	22.3

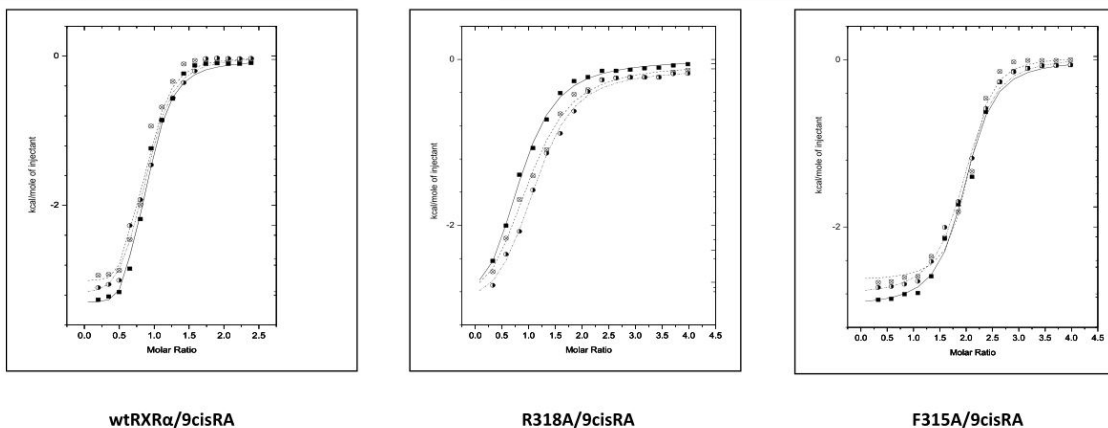


**Figure 7. Subtracted thermograms of wt-hRXR and R318A and F315A titrations in the presence of DHA**

DHA showed a dissociation constant for K1 of 2.6nM, while its K2 value was 1.1 $\mu$ M. Thermodynamically, DHA shows a higher enthalpy in its first binding site than 9cisRA (-3.88 vs -2.9 kcal/mol) while the changes in entropy were close (25.9 vs 23.3 cal/mol/deg C $^{\circ}$ ). In the R318A mutant the tetramer is prevented from dissociating upon ligand binding. The measured dissociation constant for binding of DHA drops significantly from 2.65nM to 98.4 $\mu$ M. The change in enthalpy also drops significantly to -1.65 kcal/mol. The change in entropy value remains fairly consistent at 20.8 cal/mol/deg C $^{\circ}$ .

In the F315A mutant the tetrameric conformation is prevented from forming regardless of whether or not an agonist is present. The  $K_d$  is close to constant, while the enthalpy of dissociation increased from -1.439 to -2.44 kcal/mol. The 9cisRA isotherm (see Figure 8) lacked two clearly distinguishable binding phases suggesting that  $K_1 < K_2$ .

Protein/Ligand	wtRXR $\alpha$ /9cisRA	R318A/9cisRA	F315A/9cisRA
$K_d$ - T (M)	$2.31E-07 \pm 1.2E-07$	$1.67E-06 \pm 2.4E-06$	N/A
$\Delta H$ - T (kcal/mol)	$-2.91 \pm 0.030$	$-2.72 \pm .077$	N/A
$\Delta S$ - T (cal/mol/deg)	23.3	14.9	N/A
$K_d$ - D (M)	$2.34E-08 \pm 1.4E-08$	N/A	$5.30E-07 \pm 2.9E-06$
$\Delta H$ - D (kcal/mol)	$-2.22 \pm 0.12$	N/A	$-5.83 \pm .037$
$\Delta S$ - D (cal/mol/deg)	18.0	N/A	9.24



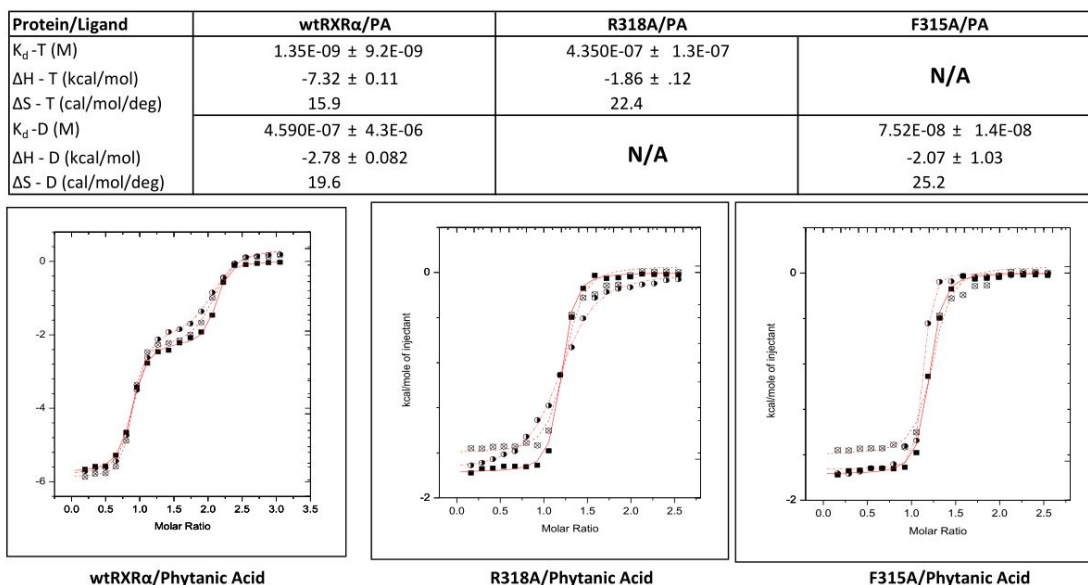
**Figure 8. Subtracted thermograms of wt-hRXR and R318A and F315A titrations in the presence of 9-*cis*-Retinoic Acid**

The ITC data alone does not show two clear distinct binding phases. However, when viewed in conjunction with our Native-PAGE data which showed the presence of both tetrameric and dimeric forms in the presence of 9cisRA along with the fact that the data was a poor fit for single binding site equilibrium, prompted us to hypothesize that wt-RXR does exhibit two site binding.

9cisRA showed an initial dissociation constant of 2.3 $\mu$ M for the tetrameric form of RXR while it showed a much stronger affinity for dimeric form (23.4nM). The R318A

mutant showed the weakest affinity for 9cisRA with a dissociation constant of 16.7  $\mu\text{M}$  while the F315A mutant had a higher affinity at 530nM

The phytanic acid binding isotherm (See Figure 9) for wt-RXR clearly showed two phases where  $K_1 > K_2$  similar to DHA with two binding states as in DHA.



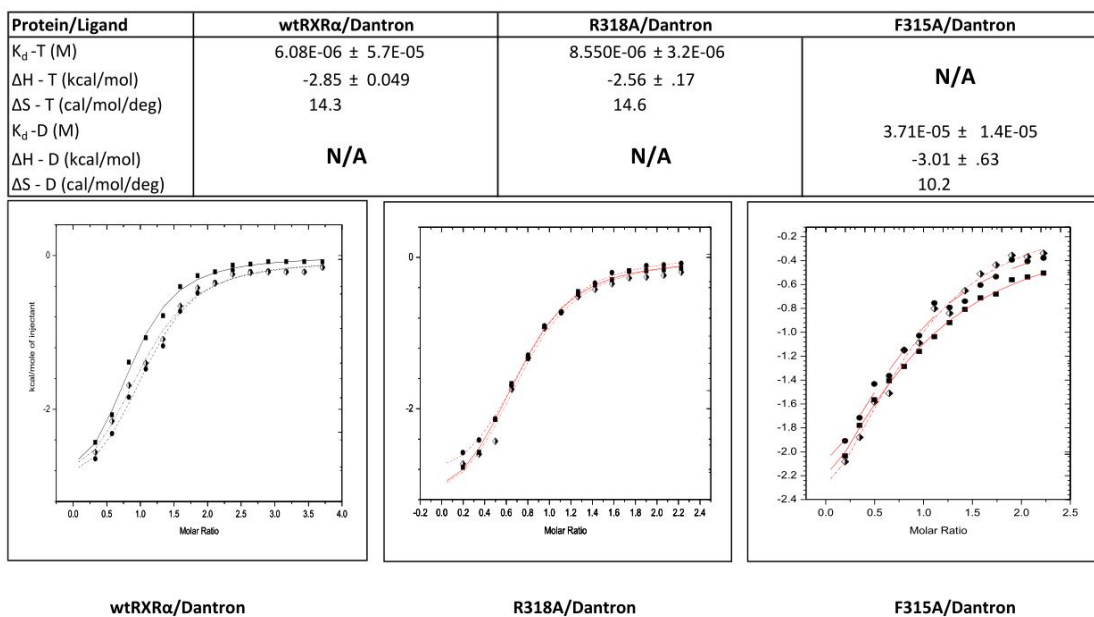
**Figure 9. Subtracted thermograms of wt-hRXR and R318A and F315A titrations in the presence of Phytanic Acid**

The ligand showed a dissociation constant for  $K_1$  of 1.35 nM, while its  $K_2$  value was 4.5 $\mu\text{M}$ . Thermodynamically, it shows an enthalpy value of -7.34 kcal/mol in its first binding while the entropy value changes from 15.9 to 19.6 cal/mol/deg  $^{\circ}\text{C}$ . In the R318A mutant the tetramer is prevented from dissociating upon ligand binding. This caused the dissociation constant for binding of phytanic acid to drop from 1.35nM to 4.3 $\mu\text{M}$ . The enthalpy of dissociation also drops significantly to -1.861 kcal/mol. The change in entropy value remains fairly consistent at 22.4 cal/mol/deg  $^{\circ}\text{C}$ .



In the F315A mutant the tetrameric conformation is prevented from forming regardless of whether or not an agonist is present. The  $K_d$  is changes to 75.2 $\mu$ M, while the change in enthalpy decreased to -2.07 kcal/mol.

Titration with a RXR antagonist, Dantron, does not show a two site model, instead fitting to a single site model with a 1:2 macromolecule to ligand stoichiometry. Danthron was found to have a dissociation constant of 11 $\mu$ M, while thermodynamically it was found to bind in a more  $\Delta S$  driven manner, with a smaller contributions from  $\Delta H$ . The R318A mutant showed an even stronger affinity for Dantron than the wild type while the F315A mutant showed a very weak low millimolar affinity (3.71mM).



**Figure 10. Subtracted thermograms of wt-hRXR and R318A and F315A titrations in the presence of DHA**

Both DHA and PA showed indications of positive co-operativity between the binding sites in contrast to our earlier assumptions. This will be discussed further in the next chapter.

**Modeling the RXR-LBD Tetramer Formation:** The next portion of the study looked to establish a model for formation of the RXR-LBD tetramer and to define the formation and dissolution of the tetramer both by its kinetic and thermodynamic parameters. Throughout this section reference is made to both total monomeric units present and monomers present. It is important for clarity to distinguish between the two. When monomers are referred to only RXR-LBD's existing in a monomeric state are meant. In contrast total monomeric units refer to the amount of RXR-LBD monomers present in any multimeric state. So a RXR tetramer would contribute 4 monomers to the total monomeric units present, for example. For this dissertation total monomeric units will typically be referred to as a concentration in molarity, as indicated by the brackets around its symbol.

As discussed earlier both previous studies<sup>4</sup> and our own work have shown that RXR-LBD can exist in three multimeric states, a monomer, a dimer, and a tetramer. It was hypothesized that the likely equilibriums system to represent the distribution and formation of each RXR-LBD multimeric states could be written as below



The above model was picked for our initial studies as it represents the simplest model for RXR multimerization. While other models could be written which all contain more complex relationships there exists no evidence currently in the literature to support their

existence over the simpler, more streamlined system. Using the above model we can then define the dissociation constants for each multimer:

**Equation 5.1)** 
$$K_d^D = \frac{[M]^4}{[D]^2}$$

**Equation 5.2)** 
$$K_d^T = \frac{[D]^2}{[T]}$$

With these definitions we can define the total equivalent concentration of RXR monomeric units ( $[M]_{T,i}$ ) within the ITC cell after any injection. First we define the initial relationship between  $[M]_{T,i}$  and each dimeric form:

**Equation 6)** 
$$[M]_{T,i} = [M] + 2[D] + 4[T]$$

Next the above definitions are rewritten in Equation 4 in terms of the dimer and tetramer concentrations only, since these two values are readily measurable from Native-PAGE experiments:

**Equation 7)** 
$$[M]_{T,i} = \sqrt[4]{K_d^D [D]^2} + 2\sqrt{K_d^T [T]} + 4[T]$$

For further derivations see appendix 1.

With ITC we measure the heat energy gained or released per injection ( $q_i$ ) which can be defined as a function of the concentration of all monomeric units ( $[M]_{Tot,i}$ ) added to the sample cell with each injection :

**Equation 8)** 
$$q_i = f([M]_{T,i})$$

Since this analysis requires the change in heat due to the aggregate macromolecules injected only and not any heat released to dissociation or association of already present macromolecules we can define the net heat released with each injection as below. The

net heat change per injection is the total heat content of multimer units contained in the injection volume minus the difference in the heat content of all protein aggregates present after and before the injection in the sample cell.

**Equation 9)** 
$$q_{i,net} = q_{syr} - (q_i - q_{i-1})$$

The heat content of a total aggregate any total aggregate population can be defined as such:

**Equation 10.1)** 
$$q_i = n_i * \Delta H$$

**10.2)** 
$$q_{i-1} = n_{i-1} * \Delta H$$

**10.3)** 
$$q_{syr} = n_{syr} * \Delta H$$

Since the proposed model cites three states in which RXR can exist, there are two transitions which contribute to heat change with each injection. To account for the contribution of each the mole fractions ( $F_D$  for the dimeric fraction or  $F_T$  for the tetrameric fraction) of each multimer is calculated (See Appendix 1). These allow the distribution of the total number of monomeric units between each state to be quantified. Since any given mole fraction can vary from zero to one, where a zero value means the given species is not present to one where the species in question is the only species present, we can use the product of each mole fraction with the specific changes in enthalpy to quantify the contribution of each transition to the total heat content (See Appendix 2 for full derivation).

**Equation 11.1)**  $q_i = [M]_{Tot,i} * V(F_{D,i}\Delta H_D + F_{T,i}\Delta H_T)$

**11.2)**  $q_{i-1} = [M]_{Tot,i-1} * V(F_{D,i-1}\Delta H_D + F_{T,i-1}\Delta H_T)$

**11.3)**  $q_{syr} = [M]_{Tot,syr} * \Delta v(F_{D,syr}\Delta H_D + F_{T,syr}\Delta H_T)$

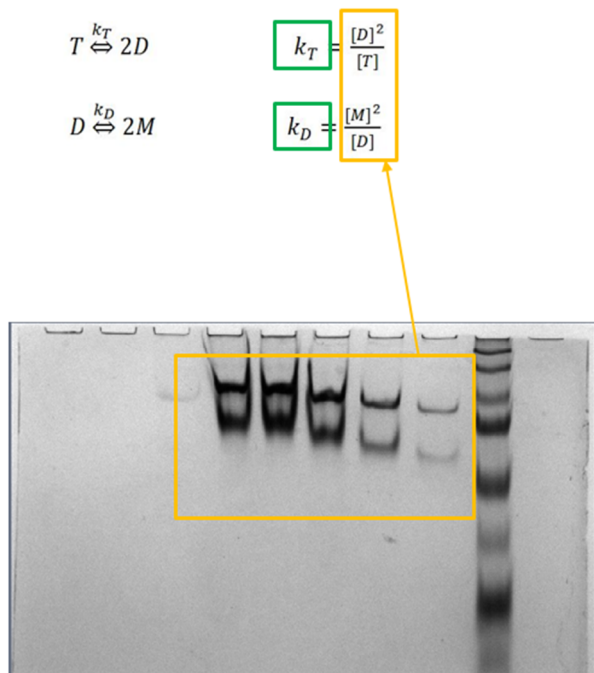
Substituting in equation 10.1-10.3 into equation 8 the heat released after the *i*-th injection can be written as follows:

**Equation 12)**  $q_{i,net} = [M]_{Tot,syr} * \Delta v(F_{D,syr}\Delta H_D + F_{T,syr}\Delta H_T) -$   
 $[[M]_{Tot,i} * V(F_{D,i}\Delta H_D + F_{T,i}\Delta H_T) - [M]_{Tot,i-1} * \Delta v(F_{D,i-1}\Delta H_D + F_{T,i-1}\Delta H_T)]$

The final step is to incorporate a dilution factor to account for volume lost from the cell each injection<sup>42</sup>:

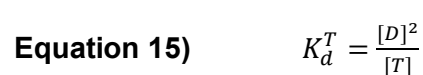
**Equation 13)**  $q_{i,net} = [M]_{Tot,syr} * \Delta v(F_{D,syr}\Delta H_D + F_{T,syr}\Delta H_T) -$   
 $[[M]_{Tot,i} * V(F_{D,i}\Delta H_D + F_{T,i}\Delta H_T) - [M]_{Tot,i-1} * \Delta v(F_{D,i-1}\Delta H_D + F_{T,i-1}\Delta H_T)] \left[ V + \frac{\Delta v}{2} \right]$

This leaves a model system where the dependent variable  $q_{i,net}$  exists as a function of total monomeric units ( $M_{Tot,i}$ ) with equilibrium constants and changes in enthalpy for each injection as parameters. The equilibrium constants can be determined from the Native-PAGE assay's while total protein present ( $M_{Tot,i}$ ) and cell volume  $V$  are known (Figure 11). Both change in enthalpy values are left as unknowns. The two unknown parameters are solved by using non-linear curve fitting analysis. Initial "guesses" are assigned to both enthalpy values and the generated curve is compared to the experimental data. By varying the values through iterative fitting and comparing the fit of the theoretical model to experimental data, values are assigned to both parameters.



**Figure 11. Native PAGE Determination of Equilibrium Constants** Native PAGE determination of the relative concentrations of the different RXR multimeric states at different concentration lvls. This allows calculation of the different dissociation equilibrium

Native-PAGE analysis showed that often the levels of RXR monomer present are either extremely low or too low for detection by standard staining techniques. This led to questions as to whether the contributions of the monomer form are small enough as to be negligible. If so a simpler equilibrium expression could be used to model the RXR tetramer formation. Therefore as well as the 3 state equilibrium model proposed above a simple 2 stage equilibrium model ignoring the contributions of the monomer as negligible was investigated. This equilibrium can be written as follows:



The total equivalent monomer concentration after any injection can be written as follows:

**Equation 16)** 
$$[M]_{T,i} = 2[D] + 4 \frac{[D]^2}{K_d^T}$$

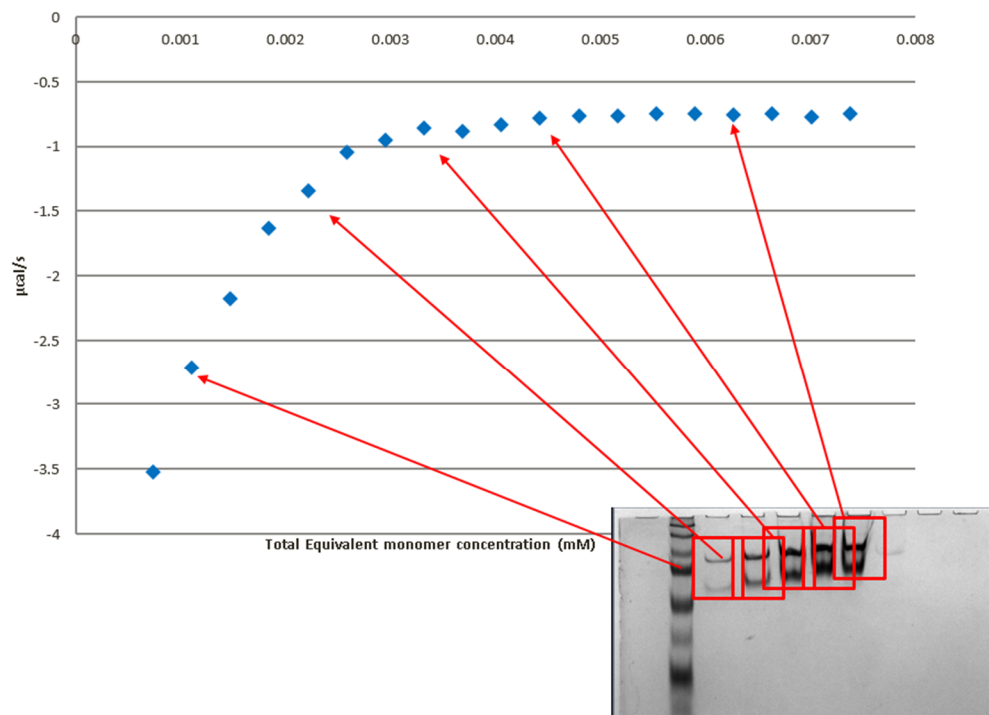
The heat released each injection can then be written (see *ITC data analysis in Origin*, 2001 for derivation)<sup>42</sup>:

**Equation 17)** 
$$q_{i,net} = [M]_{Tot,syr} * \Delta v(\Delta H_T) - V\Delta H_T([M]_{T,i} - [M]_{T,i-1}) \left( V + \frac{\Delta v}{2} \right)$$

Where V is the volume of the sample cell and Δv is the injection volume. Once again we are have a system where q<sub>i</sub> is a function of [M]<sub>T,i</sub>. Using non-linear curve fitting analysis along with our Native-PAGE analysis we can assign values to both the dissociation constant and change in enthalpy for the dissociation of RXR tetramers into dimers.

The process of fitting experimental data then involves four parts. First initial guesses (often these can be made accurately enough by the Origin fitting software) of each K, and ΔH parameter are made. The second is calculations of q<sub>i</sub> for each injection using the initial guesses. This calculated value is compared with the measured heat for the corresponding experimental injection. Third is improvement of the initial parameters by the standard Marquardt methods (for a good review of this method see *The Levenberg-Marquardt method for nonlinear least squares curve-fitting problems*, Gavin 2013) and finally iteration of the above steps until no further significant improvement in the fit occurs.

Non-denaturing Native-PAGE analysis was used to quantify the distribution of the different RXR multimer states at different concentrations. By matching the total protein added to specific lanes of a gels to the amount of protein present after a certain number of injections in the ITC assay's a "snapshot" of the multimer distribution after the injections in question was obtained.



**Figure 12. Native-PAGE modeling of multimeric states within ITC sample cell.** By matching the concentrations of different lanes of the each gel to the known sample cell concentration after selected ITC injections, the concentration of each multimer can be determined.

Two sets of three Native-Page experiments were performed (see Appendix **4a-b** for full data). Each set was paired with a set of partner ITC assays. Each set of paired PAGE and ITC assays was performed with the same batch of purified recombinant protein to ensure that there was no difference in activity due to differences in protein lots.

The first set was performed for 15 1.5µL injections of purified RXR protein into a sample cell containing only dialyzed sample buffer. RXR was added to lanes 2-6 in concentrations to match the total protein present in the cell after the injections number 2, 5, 8, 11 and 14 respectively.

The second set was done with 20 1 µL injections. By varying our methodology with different injections sizes we could ensure that protein aggregation was not



adversely affecting our measurements. If aggregation is not an issue our values for  $K_D$  and  $\Delta H$  should be consistent across the 1  $\mu\text{L}$  and 1.5  $\mu\text{L}$  experiments.

For each Native-P AGE experiment an average  $K_d$  for each transition (2 in our first model, 1 in the second) was calculated. For both proposed models heat released per injection was defined as a function of total monomeric units injected,  $q_i = f([M]_{T,i})$ .

Using the non-linear curve fitting analysis built in to the specialized Origin 7.0 software provided with the ITC iterative fitting was used to assign values to  $\Delta H_D$  and  $\Delta H_T$  for model one or to  $\Delta H_T$  for the second simpler model. The fit for each set of calculated data to the experimental data set was measured by  $\chi^2$  analysis.

## CHAPTER IV

### DISCUSSION AND CONCLUSIONS

**Ligand Binding Study:** Analysis of the ITC data on the interaction of RXR ligand binding domain with agonist and antagonist ligands supports the original hypothesis. It was postulated that the DHA and phytanic acid, being fatty acids able to adopt multiple molecular conformations would show a better ability to interact with both the "I" and "L" conformations of the RXR ligand binding pocket, while 9cisRA with its more rigid retinoid structure would show a preference for the "L" conformation over the "I". Both the wild type and mutant binding assay results support this prediction.

*wt*-RXR demonstrated a higher K1 binding affinity than K2 when binding the fatty acids. This may reflect the fact that unbound DHA molecules preferentially bind to tetrameric RXR over the dimeric form of the receptor. This would fit with the literature that speculate that the tetrameric form of RXR serves an autorepressive. However, 9cisRA showed a lower affinity for K1 to K2 vs DHA. In these assays as dimeric RXR preferentially bound 9cisRA, binding to and dissociating RXR tetramers when the dimeric partners were all fully bound already. Further investigation with both the R318A and F315A mutants further supported our hypothesis. DHA showed similar binding to both the R318A and F315A mutants while the decreased binding of 9cisRA to the F315A mutant is further evidence that the retinoid has weaker interactions with the tetrameric "I" binding pocket. This is consistent with the growing trend in the literature

which shows increased links between DHA and fatty acids to both retinoid and RXR requiring heterodimeric partner NRs.<sup>33 37, 43</sup> As previously noted there is some evidence of cooperativity between binding sites in *wt*-RXR.

Of particular interest are the data showing that DHA binds to RXR with a much higher affinity than has been suggested from previous gene activation and cell culture assay's would have suggested. Previous studies have shown EC50 and activation constants in the low micromolar range for DHA while these data showed that DHA physically binds to the receptor with a low nanomolar dissociation constant. While initially this seems like a large discrepancy, when one considers the nature of the RXR autorepression mechanism this difference makes sense. RXR monomers have been shown to have the ability to heterodimerize and activate gene expression regardless of ligand binding. Hence, the autorepressive function of the RXR tetramer which sequesters the monomer into an oligomeric state where they are transcriptionally active.

Previous studies have shown that both the presence of a bound ligand and the nature of the ligand itself can affect whether a monomer is predisposed to homo- or heterodimerize as well as predispose the monomer to certain heterodimeric partners over others<sup>21 19</sup>. Therefore, it is reasonable that an RXR ligand would bind and dissociate the RXR tetramer while only partially activating the homodimerization function, leaving a pool of RXR monomers available to heterodimerize and activate other pathways.

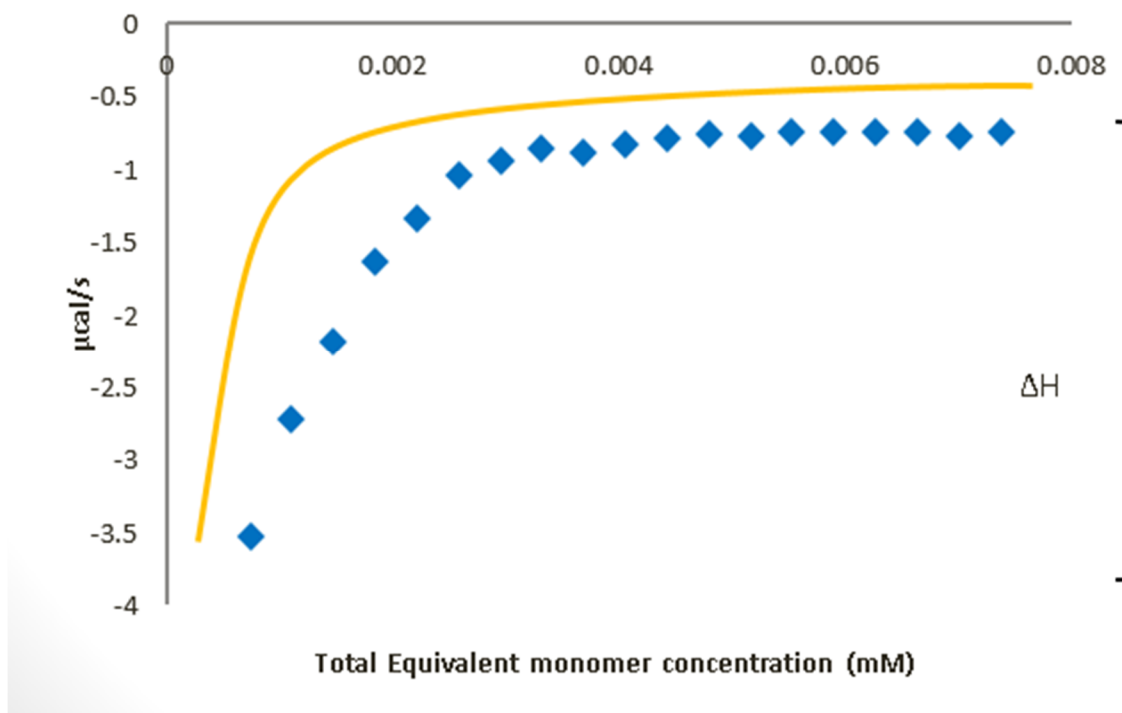
Looking at the thermodynamics of the ligand binding seen in the assays, two trends became noticeable. Firstly,  $\Delta H$  values appear to be linked to changes in the multimeric state of the receptor. Binding events which induce no change between dimer, tetramer or monomer, such as binding of Danthron to *wt*-RXR or binding to the R318A

mutant, where found to consistently have smaller changes in enthalpy vs. assay's where a change in multimeric state occurs. In contrast  $\Delta S$  values are similar across all binding events, not matter the dissociation or association events occurring. We can draw two conclusions from this. Firstly that the protein-protein interactions are largely  $\Delta H$  driven. Also ligand binding by RXR is largely  $\Delta S$  driven, not surprising given the heavily hydrophobic nature of RXR ligand molecules.

The final thermodynamic observation is between the two fatty acids, DHA and phytanic acid. The major difference between the two is the presence of 4 methyl groups on phytanic acid's main aryl chain while DHA contains none. This lead to large variations in the enthalpy values with phytanic acid between the different RXR wild type and mutant forms than was seen in DHA though both showed similar kinetic binding constants. Looking at this, the conclusion is drawn that phytanic acid seems to bind in an even more  $\Delta S$  driven manner than DHA due to its bulky structure.

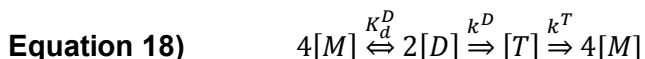
**Tetramer Dissociation Modeling:** In analyzing the RXR dissociation data obtained in the absence of ligand two features where looked at beyond goodness of the fit as measured by the  $\chi^2$  minimization. For the theoretical dissociation curves produced, two features also where noted. Rate of change for  $q_i$  vs  $[M]T,i$  and any inflections point seen are influenced by the values of the equilibrium constants while the magnitude of  $q_i$  is related to the values of the  $\Delta H$  components. By comparing these qualities of our fitted models to the experimentally generated curves even for data sets which fail to fit we can make observations of how our model differs from our experimental data. The results are as follows:

For both models, the monomer-dimer-tetramer and the dimer-tetramer, we failed to generate a solution for the assigned parameters which fit to our experimental data. All sets showed a reduced  $\chi^2$  value reflecting a “good” fit to our experimental data. However in comparing the “best fit” , or reduced solutions  $\chi^2$  generated for the model consisting of a monomer-dimer-tetramer equilibrium it was noted that the error in our model was associated primarily in the parameters related to change in enthalpy. When comparing the generated model to the experimental data it was found that the 3 state model accurately reflected the experimental data but predicted less heat released for each injection than was actually observed (See Figure 11).



**Figure 13. Partially Fitted Model of 3 State RXR Equilibrium** The 3 state model we proposed for RXR tetramer dissociation (in yellow) vs our experimental ITC data (blue data points)

Reviewing the data from initial multimer studies, the data showed that while the RXR tetramer dissociation is a multi-stage process it is more exothermic than a simple monomer-dimer-tetramer equilibria should be. The most likely explanation for this would be that one of the transitions between multimers features a greater number of sub-units dissociating/associating than our original model called for. In order to expand our model, the literature was consulted. Previous studies (Kersten (2001), Kersten (2004), Zhang cite) agree that tetramer's most likely biological function is to sequester RXR monomers, preventing them from being available for homo- and heterodimeric functions. With the biological function in mind, as well as the previous observations from our rejected earlier model, it is hypothesized that a more complete model for RXR tetramer dissociation and formation would be as follows:



The dissociation of the tetramer directly to four monomeric units in this model should address the larger energy releases than expected which were observed. One key difference is that since in this model tetramer association and dissociation are one not reversible each of these two transition is defined by a rate constant,  $k$ , instead of an equilibrium dissociation constant,  $K_d$ , as in previous models. Since to determine the rate constants of tetramer dissociation and formation are beyond the scope of our ITC and Native-PAGE methodology the equation for total equivalent monomer concentration ( $[M]_{T,i}$  in terms of each multimeric state as known non-denaturing gel assays can be kept in its simplified form. For this model  $[M]_{T,i}$  is defined as follows:



Determination of rate constants is not possible with our existing ITC methodology as was possible for equilibrium constants. Devising a methodology to determine them is beyond the scope of this study. [M], [D] and [T] can be determined from native-PAGE assays as described earlier.

From here we now look to define our heat release per injection as for the previous models. Again, heat per injection is defined a function of change in total equivalent monomer concentration after the injection and before it.

**Equation 20)**  $q_i = f([M]_{T,i})$

As before the difference in the total heat equivalent for of all contents of the cell before and after the injection in question were calculated. Each heat equivalent is equal to the sum of formation of multimer, define as a product of the total monomer concentration, the mole fraction of the multimer in question and the change in enthalpy associated with that transition as in the original model. The final equation for heat released per injection,  $q_i$ , is:

**Equation 21)**  $q_i = [V[M]_{T,i}(F_M\Delta H_M + F_{D,i}\Delta H_D + F_{T,i}\Delta H_T) + V[M]_{T,i-1}(F_{M-1}\Delta H_{M-1} + F_{D,i-1}\Delta H_D + F_{T,i-1}\Delta H_T)] \left[ V + \frac{dV_i}{2} \right]$

As more subunits are dissociating simultaneously in the tetramer to monomer step of this model a greater change in enthalpy per dissociating tetramer is predicted. This should address the failing of the original dissociation model. This model is currently under evaluation as to whether it accurately reflects the obtained experimental data.

**Future Directions:** From here there are several avenues available for future exploration. The first would be the use of full length hRXR $\alpha$  in these studies instead of the LBD by itself. This could allow for ITC studies to include binding to short oligonucleotide fragments containing known or suspected RXR REs.

A second step would be the addition of different nuclear receptors known to heterodimerize with RXR. PPAR, LXR and VDR for example have been previously shown to have their activity levels modified in mouse models when known RXR agonists are administered.<sup>45 46</sup> By including these at different stages of ITC assays it should be possible to see an increase or decrease in RXR complex formation depending on the ligand or mutant form of RXR used.

Finally, testing of the final model of RXR tetramer dissociation proposed in this dissertation. If the model does fit to the experimental data obtained the next step will be elucidation of the rate constants which govern tetramer dissociation to monomers or association from dimers. One possible avenue for exploring this would be the use of FRET studies and fluorescent tagged RXR-LBD. By using real-time monitoring of changes in fluorescence as LBDs associate and dissociate it should be possible to measure the rates of tetramer dissociation and association.



## WORKS CITED

1. Olefsky, J. M., Nuclear receptor minireview series. *J Biol Chem* **2001**, 276 (40), 36863-4.
2. Moore, J. T.; Collins, J. L.; Pearce, K. H., The nuclear receptor superfamily and drug discovery. *ChemMedChem* **2006**, 1 (5), 504-23.
3. Germain, P.; Chambon, P.; Eichele, G.; Evans, R.; Lazar, M.; Leid, M.; De Lera, A.; Lotan, R.; Mangelsdorf, D.; Gronemeyer, H., International Union of Pharmacology. LXIII. Retinoid X receptors. *Pharmacol Rev* **2006**, 58 (4), 760-72.
4. Kersten, S.; Kelleher, D.; Chambon, P.; Gronemeyer, H.; Noy, N., Retinoid X receptor alpha forms tetramers in solution. *Proc Natl Acad Sci U S A* **1995**, 92 (19), 8645-9.
5. Mangelsdorf, D.; Borgmeyer, U.; Heyman, R.; Zhou, J.; Ong, E.; Oro, A.; Kakizuka, A.; Evans, R., Characterization of three RXR genes that mediate the action of 9-cis retinoic acid. *Genes Dev* **1992**, 6 (3), 329-44.
6. Kersten, S.; Pan, L.; Noy, N., On the role of ligand in retinoid signaling: positive cooperativity in the interactions of 9-cis retinoic acid with tetramers of the retinoid X receptor. *Biochemistry* **1995**, 34 (43), 14263-9.
7. Thacher, S. M.; Vasudevan, J.; Chandraratna, R. A., Therapeutic applications for ligands of retinoid receptors. *Curr Pharm Des* **2000**, 6 (1), 25-58.
8. Goldstein, J.; Dobrzyn, A.; Clagett-Dame, M.; Pike, J.; DeLuca, H., Isolation and characterization of unsaturated fatty acids as natural ligands for the retinoid-X receptor. *Arch Biochem Biophys* **2003**, 420 (1), 185-93.

9. Heyman, R.; Mangelsdorf, D.; Dyck, J.; Stein, R.; Eichele, G.; Evans, R.; Thaller, C., 9-cis retinoic acid is a high affinity ligand for the retinoid X receptor. *Cell* **1992**, *68* (2), 397-406.
10. Zhang, H.; Zhou, R.; Li, L.; Chen, J.; Chen, L.; Li, C.; Ding, H.; Yu, L.; Hu, L.; Jiang, H.; Shen, X., Danthron Functions as a Retinoic X Receptor Antagonist by Stabilizing Tetramers of the Receptor. *J. Biol. Chem.* **2011**, *286* (3), 1868-1875.
11. Gampe, R. T.; Montana, V. G.; Lambert, M. H.; Wisely, G. B.; Milburn, M. V.; Xu, H. E., Structural basis for autorepression of retinoid X receptor by tetramer formation and the AF-2 helix. *Genes Dev* **2000**, *14* (17), 2229-41.
12. Chawla, A.; Repa, J. J.; Evans, R. M.; Mangelsdorf, D. J., Nuclear receptors and lipid physiology: opening the X-files. *Science* **2001**, *294* (5548), 1866-70.
13. Pelton, P. D.; Patel, M.; Demarest, K. T., Nuclear receptors as potential targets for modulating reverse cholesterol transport. *Curr Top Med Chem* **2005**, *5* (3), 265-82.
14. Rastinejad, F.; Perlmann, T.; Evans, R. M.; Sigler, P. B., Structural determinants of nuclear receptor assembly on DNA direct repeats. **1995**, *375* (6528), 203-211.
15. Bain, D. L.; Heneghan, A. F.; Connaghan-Jones, K. D.; Miura, M. T., Nuclear receptor structure: implications for function. *Annu Rev Physiol* **2007**, *69*, 201-20.
16. The nuclear receptor ligand-binding domain: structure and function. **1998**, *10* (3), 384-391.
17. Mangelsdorf, D. J.; Thummel, C.; Beato, M.; Herrlich, P.; Schutz, G.; Umesono, K.; Blumberg, B.; Kastner, P.; Mark, M.; Chambon, P.; Evans, R. M., The nuclear receptor superfamily: the second decade. *Cell* **1995**, *83* (6), 835-9.
18. Kersten, S.; Dong, D.; Lee, W.-Y.; Reczek, P. R.; Noy, N., Auto-silencing by the retinoid X receptor. *J. Mol. Biol.* **1998**, *284* (1), 21-32.

19. Kersten, S.; Gronemeyer, H.; Noy, N., The DNA binding pattern of the retinoid X receptor is regulated by ligand-dependent modulation of its oligomeric state. *J Biol Chem* **1997**, *272* (19), 12771-7.
20. Zhang, H.; Li, L.; Chen, L.; Hu, L.; Jiang, H.; Shen, X., Structure Basis of Bigelovin as a Selective RXR Agonist with a Distinct Binding Mode. *J. Mol. Biol.* **2011**, *407* (1), 13-20.
21. Vivat-Hannah, V.; Bourguet, W.; Gottardis, M.; Gronemeyer, H., Separation of retinoid X receptor homo- and heterodimerization functions. *Mol Cell Biol* **2003**, *23* (21), 7678-88.
22. Bourguet, W.; Ruff, M.; Chambon, P.; Gronemeyer, H.; Moras, D., Crystal structure of the ligand-binding domain of the human nuclear receptor RXR-alpha. *Nature* **1995**, *375* (6530), 377-82.
23. Zhang, X.-K.; Salbert, G.; Lee, M.-O.; Pfahl, M., Mutation that alter ligand-induced switches and dimerization activities in the retinoid X receptor. *Mol. Cell. Biol.* **1994**, *14* (6), 4311-23.
24. Boehm, M.; Zhang, L.; Zhi, L.; McClurg, M.; Berger, E.; Wagoner, M.; Mais, D.; Suto, C.; Davies, J.; Heyman, R., Design and synthesis of potent retinoid X receptor selective ligands that induce apoptosis in leukemia cells. *J Med Chem* **1995**, *38* (16), 3146-55.
25. Yan, X.; Perez, E.; Leid, M.; Schimerlik, M. I.; De Lera, A. R.; Deinzer, M. L., Deuterium exchange and mass spectrometry reveal the interaction differences of two synthetic modulators of RXR alpha LBD. *Protein Science* **2007**, *16* (11), 2491-2501.

26. Shulman, A.; Larson, C.; Mangelsdorf, D.; Ranganathan, R., Structural determinants of allosteric ligand activation in RXR heterodimers. *Cell* **2004**, *116* (3), 417-29.
27. Levin, A. A.; Sturzenbecker, L. J.; Kazmer, S.; Bosakowski, T.; Huselton, C.; Allenby, G.; Speck, J.; ratzeisen, C.; Rosenberger, M.; Lovey, A.; Grippo, J. F., 9-Cis retinoic acid stereoisomer binds and activates the nuclear receptor RXR[alpha]. *Nature* **1992**, *355* (6358), 359-361.
28. Yu, V. C.; Delsert, C.; Andersen, B.; Holloway, J. M.; Devary, O. V.; Naar, A. M.; Kim, S. Y.; Boutin, J. M.; Glass, C. K.; Rosenfeld, M. G., RXR beta: a coregulator that enhances binding of retinoic acid, thyroid hormone, and vitamin D receptors to their cognate response elements. *Cell* **1991**, *67* (6), 1251-66.
29. Durand, B.; Saunders, M.; Leroy, P.; Leid, M.; Chambon, P., All-trans and 9-cis retinoic acid induction of CRABP II transcription is mediated by RAR-RXR heterodimers bound to DR1 and DR2 repeated motifs. *Cell* **1992**, *71* (1), 73-85.
30. Leid, M., Ligand-induced alteration of the protease sensitivity of retinoid X receptor alpha. *J Biol Chem* **1994**, *269* (19), 14175-81.
31. Urbach, J.; Rando, R. R., Isomerization of all-trans-retinoic acid to 9-cis-retinoic acid. *Biochem J* **1994**, *299* ( Pt 2), 459-65.
32. Calléja, C.; Messaddeq, N.; Chapellier, B.; Yang, H.; Krezel, W.; Li, M.; Metzger, D.; Mascrez, B.; Ohta, K.; Kagechika, H.; Endo, Y.; Mark, M.; Ghyselinck, N.; Chambon, P., Genetic and pharmacological evidence that a retinoic acid cannot be the RXR-activating ligand in mouse epidermis keratinocytes. *Genes Dev* **2006**, *20* (11), 1525-38.

33. de Urquiza, A. M.; Liu, S.; Sjöberg, M.; Zetterström, R. H.; Griffiths, W.; Sjövall, J.; Perlmann, T., Docosahexaenoic acid, a ligand for the retinoid X receptor in mouse brain. *Science* **2000**, *290* (5499), 2140-4.
34. Zapata-Gonzalez, F.; Rueda, F.; Petriz, J.; Domingo, P.; Villarroya, F.; Diaz-Delfin, J.; de Madariaga, M. A.; Domingo, J. C., Human dendritic cell activities are modulated by the omega-3 fatty acid, docosahexaenoic acid, mainly through PPAR $\gamma$ : RXR heterodimers: comparison with other polyunsaturated fatty acids. *J. Leukocyte Biol.* **2008**, *84* (4), 1172-1182.
35. Wietrzych-Schindler, M.; Szyszka-Niagolov, M.; Ohta, K.; Endo, Y.; Perez, E.; de Lera, A. R.; Chambon, P.; Krezel, W., Retinoid X Receptor Gamma Is Implicated in Docosahexaenoic Acid Modulation of Despair Behaviors and Working Memory in Mice. *Biol. Psychiatry* **2011**, *69* (8), 788-794.
36. German, O. L.; Monaco, S.; Agnolazza, D. L.; Rotstein, N. P.; Politi, L. E., Retinoid X receptor activation is essential for docosahexaenoic acid protection of retina photoreceptors. *J Lipid Res* **2013**, *54* (8), 2236-46.
37. Yakunin, E.; Loeb, V.; Kisos, H.; Biala, Y.; Yehuda, S.; Yaari, Y.; Selkoe, D. J.; Sharon, R., Alpha-synuclein neuropathology is controlled by nuclear hormone receptors and enhanced by docosahexaenoic acid in a mouse model for Parkinson's disease. *Brain Pathol* **2012**, *22* (3), 280-94.
38. Elmazar, M. M.; Nau, H., Potentiation of the teratogenic effects induced by coadministration of retinoic acid or phytanic acid/phytol with synthetic retinoid receptor ligands. *Arch Toxicol* **2004**, *78* (11), 660-8.
39. Nagpal, S.; Yang, Z.; Morris, E.; Lavallie, E.; Collins-Racie, L. A. Use of RXR agonists for the treatment of osteoarthritis. 2009-US33795

2009102789, 20090211., 2009.

40. Schluter, A.; Yubero, P.; Iglesias, R.; Giralt, M.; Villarroya, F., The chlorophyll-derived metabolite phytanic acid induces white adipocyte differentiation. *Int J Obes Relat Metab Disord* **2002**, 26 (9), 1277-80.
41. Ladbury, J. E., Calorimetry as a tool for understanding biomolecular interactions and an aid to drug design. *Biochem Soc Trans* **2010**, 38 (4), 888-93.
42. Velazquez-Campoy, A.; Leavitt, S. A.; Freire, E., Characterization of protein-protein interactions by isothermal titration calorimetry. *Methods Mol Biol* **2004**, 261, 35-54.
43. Wietrych-Schindler, M.; Szyszka-Niagolov, M.; Ohta, K.; Endo, Y.; Perez, E.; de Lera, A. R.; Chambon, P.; Krezel, W., Retinoid x receptor gamma is implicated in docosahexaenoic acid modulation of despair behaviors and working memory in mice. *Biol Psychiatry* **2011**, 69 (8), 788-94.

**APPENDIX A**  
**DERIVATIONS**

#1 – Total Equivalent Monomer Concentration

$$[M]_T = [M]_F + 2[D] + 4[T] \longrightarrow \text{(eq 1)}$$

$$\#2 - [D] \xleftrightarrow{K_D} 2[M]K_D = \frac{[M]_F^2}{[D]} [D] = \frac{1}{K_D} [M]_F^2 \longrightarrow \text{(eq 2)}$$

$$\#3 - [T] \xleftrightarrow{K_T} 2[D]K_T = \frac{[D]^2}{[T]} [T] = \frac{1}{K_T} [D]^2 \longrightarrow \text{(eq 3)}$$

$$\#4 - [M]_T = [M]_F + 2[D] + \frac{4}{K_T} [D]^2 \quad \text{substitute (eq 3) into (eq 1)}$$

$$\#5 - [M]_T = [M]_F + 2 \left( \frac{1}{K_D} [M]_F^2 \right) + \frac{4}{K_T} \left( \frac{1}{K_D} [M]_F^2 \right)^2 \quad \text{substitute (eq 2) into (eq 4)}$$

$$\#6 - [M]_T = [M]_F + \frac{2}{K_D} [M]_F^2 + \frac{4}{K_T} \frac{[M]_F^4}{K_D^2} \quad \text{simplify}$$

– Mole Fraction of Dimer

$$\#7 - F_D = \frac{2[D]}{[M]_F + 2[D] + 4[T]} \quad \text{substitute (eq. 2) (eq. 6)}$$

$$\#8 - F_D = \frac{\frac{2}{K_D} [M]_F^2}{[M]_F + \frac{2}{K_D} [M]_F^2 + \frac{4}{K_T} \frac{[M]_F^4}{K_D^2}} \quad \text{(eq 8)}$$

– Mole Fraction of Tetramer

$$\#9 - F_T = \frac{4[T]}{[M]_F + 2[D] + 4[T]} \quad \text{substitute (eq. 3) (eq. 6)}$$

$$\#10 - F_T = \frac{\frac{4}{K_T} \frac{[M]_F^4}{K_D^2}}{[M]_F + \frac{2}{K_D} [M]_F^2 + \frac{4}{K_T} \frac{[M]_F^4}{K_D^2}} \quad \text{(eq 10)}$$

**Derivation of the net heat released per injection of wt-RXR $\alpha$  in the absence of ligand**

1. The net heat change per injection is the total heat content of multimer units contained in the injection volume – [the heat content of the aggregate multimer forms present after each injection - content before each injection] (see *ITC Data Analysis in Origin*, MicroCal Inc., 2004):

$$1.1. q_{i,net} = q_{syr} - (q_i - q_{i-1})$$

2. The heat due to total aggregate multimer present, whether before or after an injection is defined as (total number of RXR monomer units present (in moles)) X (enthalpy of formation):

$$2.1. q_i = n_i * \Delta H$$

$$2.2. q_{i-1} = n_{i-1} * \Delta H$$

$$2.3. q_{syr} = n_{syr} * \Delta H$$

3. Amount of aggregate present (in all forms) is equal to (concentration of total monomer units) X (sample cell volume)

$$3.1. q_i = [M]_{Tot,i} * V * \Delta H$$

$$3.2. q_{i-1} = [M]_{Tot,i-1} * V * \Delta H$$

$$3.3. q_{syr} = [M]_{Tot,syr} * \Delta v * \Delta H$$

<b><u>Parameters</u></b>	
$q_{i,net}$	Net heat change per injection (cal)
$q_{i,syr}$	Heat content of aggregates injected (cal)
$q_i$	Heat content of aggregates after injection (cal)
$q_{i-1}$	Heat content of aggregates before injection (cal)

<b><u>New Parameters</u></b>	
$n_i$	Number of monomer units in cell after injection (mol)
$n_{i-1}$	Number of monomer units in cell before injection (mol)
$n_{syr}$	Number of monomer units in injected volume (mol)
$V$	Cell volume (L)
$\Delta v$	Injection Volume (L)
$[M]_{Tot,i}$	Conc. of monomeric units after injection
$[M]_{Tot,i-1}$	Conc. of monomeric units present before injection (mol/L)
$[M]_{Tot,syr}$	Conc. of monomeric units



4. Contribution of each transition, tetramer to dimer and dimer to tetramer, to the net heat content is accounted for by use of the mole fraction of each species and each transitions unique change in enthalpy

$$4.1. q_i = [M]_{Tot,i} * V(F_{D,i}\Delta H_D + F_{T,i}\Delta H_T)$$

$$4.2. q_{i-1} = [M]_{Tot,i-1} * V(F_{D,i-1}\Delta H_D + F_{T,i-1}\Delta H_T)$$

$$4.3. q_{syr} = [M]_{Tot,syr} * \Delta v(F_{D,syr}\Delta H_D + F_{T,syr}\Delta H_T)$$

5. Substitution of 3.1, 3.2 and 3.3 into 1.1 yields

$$5.1. q_{i,net} = [M]_{Tot,syr} * \Delta v(F_{D,syr}\Delta H_D + F_{T,syr}\Delta H_T) - [[M]_{Tot,i} * V(F_{D,i}\Delta H_D + F_{T,i}\Delta H_T) - [M]_{Tot,syr} * \Delta v(F_{D,syr}\Delta H_D + F_{T,syr}\Delta H_T)]$$

6. Incorporation of a dilution factor for volume lost each injection (see *ITC Data Analysis in Origin*, MicroCal Inc., 2004 for derivation of term)

$F_{D,i}$	Mole fraction of dimer after injection
$F_{D,i-1}$	Mole fraction of dimer before injection
$F_{D,syr}$	Mole fraction of dimer in inj vol.
$F_{T,i}$	Mole fraction of tetramer after injection
$F_{T,i-1}$	Mole fraction of tetramer before injection
$F_{T,syr}$	Mole fraction of tetramer in inj vol.
$\Delta H_D$	Enthalpy of dimer/monomer transition (cal/mol)
$\Delta H_T$	Enthalpy of tetramer/dimer transition (cal/mol)

$$\begin{aligned}
 \mathbf{6.1.} \quad q_{i,net} = & [M]_{Tot,syr} * \Delta v (F_{D,syr} \Delta H_D + F_{T,syr} \Delta H_T) - [M]_{Tot,i} * V (F_{D,i} \Delta H_D + \\
 & F_{T,i} \Delta H_T) - [M]_{Tot,syr} * \Delta v (F_{D,syr} \Delta H_D + F_{T,syr} \Delta H_T) \left[ V + \frac{\Delta v}{2} \right]
 \end{aligned}$$

## APPENDIX B

### POOLED STANDARD DEVIATION

Pooled Variance ( $S_p^2$ ) is defined as:

$$1) S_p^2 = \left( \frac{(n_1-1)S_1^2 + (n_2-1)S_2^2 + \dots + (n_k-1)S_k^2}{(n_1-1) + (n_2-1) + \dots + (n_k-1)} \right)$$

Where  $n_1, n_2, \dots, n_k$  is the size of each sample set respectively.

$S_1^2, S_2^2, \dots, S_k^2$  is the variance of each sample set.

Standard Pooled Deviation ( $S_p$ ) is defined as the square root of the pooled variance:

$$2) S_p = \sqrt{S_p^2}$$

**APPENDIX C**  
**ORIGIN FITTING PROGRAM**

[GENERAL INFORMATION]

Function Name=Tetramer Dissociation

Brief Description=Dissociation of Tetramer via Dimer to monomer

Function Source=N/A

Function Type=User-Defined

Function Form=Y-Script

Number Of Parameters=4

Number Of Independent Variables=3

Number Of Dependent Variables=1

Analytical Derivatives for User-Defined=Off

[FITTING PARAMETERS]

Naming Method=User-Defined

Names=dH\_D, dH\_T, K\_T, K\_D

Meanings=?

Initial Values=--(V)

Lower Bounds=--(X,OFF)

Upper Bounds=--(X,OFF)

Number Of Significant Digits=3,2

[FORMULA]

$$NDH = M_{(Tot,syr)} * dv * (F_{(D,syr)} * dH_D + F_{(T,syr)} * dH_T) - M_{(Tot,i)} * V * (F_{(D,i)} * dH_D + F_{(T,i)} * dH_T) - M_{(Tot,i-1)} * dv * (F_{(D,i-1)} * dH_D + F_{(T,i-1)} * dH_T) + dv/2$$

[CONSTRAINTS]

/\*Enter general linear constraints here\*/

[CONSTANTS]

[Parameters Initialization]

/\*Scripts to be executed to initialize parameters.\*/

[INITIALIZATIONS]

/\*Scripts to be executed before fitting, a good place for complicated initialization.\*/

[AFTER FITTING]

%W=%H;

%Z=%H![fit.p].text\$;

%B=%[%Z,@1];

%B=%B\r\n%[%Z,@2];

```

%B=%B\r\nChi^2 = $(nlsf.chisqr,*4);

%Z="";

%Z=%Z\r\nlg(D)H (cal/mole)\t$(nlsf.p1,*4)\t(177)\$(nlsf.e1,*3);

%Z=%Z\r\nK (mM)\t$(nlsf.p2,*3)\t(177)\$(nlsf.e2,*2);

label -s -sa -n fit.p %B%Z;

SaveRedirection=type.Redirection(16,3); // SDB 1/7/99 REPORT_TO_OUTPUTLOG

type.BeginResults(); // RKM 12/10/98 v6.0141 REPORT_TO_OUTPUTLOG

type -a %B;

type -a lg(D)H (cal/mole)\t$(nlsf.p1,*4)\t$(nlsf.e1,*3);

type -a K (mM)\t$(nlsf.p2,*3)\t$(nlsf.e2,*2);

type.EndResults();

type.Redirection=SaveRedirection; // restore previous redirection.

delete -v SaveRedirection;

win -a %W;

queue {legend;}

```

[ON PARAM CHANGE]

/\*Scripts to be executed when parameters change.\*/

[INDEPENDENT VARIABLES]

xmt=

xt=

injuv=

[DEPENDENT VARIABLES]

NDH=

[CONTROLS]

General Linear Constraints=Off

Initialization Scripts=Off

Scripts After Fitting=On

Number Of Duplicates=N/A

Duplicate Offset=N/A

Duplicate Unit=N/A

Generate Curves After Fitting=No

Curve Point Spacing=Same X as Fitting Data

Generate Peaks After Fitting=Yes

Generate Peaks During Fitting=Yes

Generate Peaks with Baseline=Yes

Paste Parameters to Plot After Fitting=Yes

Paste Parameters to Notes Window After Fitting=Yes

Generate Residuals After Fitting=No

Keep Parameters=No

Enable Parameters Initialization=0

Compile On Param Change Script=23545

[COMPILE FUNCTION]

Compile=0

Compile Parameters Initialization=0

On Param Change Scripts Enabled=0



**APPENDIX D**  
**NATIVE PAGE DATA**

Definitions :

**[Syr]** – RXR-LBD conc. in the ITC syringe

**Δv** – Injection Volume (μL)

**V** – ITC Sample Cell volume (μL)

1 a	Inj #	[M] <sub>Total</sub>	[M] <sub>Monomer</sub>	[M] <sub>Dimer</sub>	[M] <sub>Tetramer</sub>	K <sub>D-T</sub>	K <sub>D-D</sub>	[Syr]	Δv	V
								5.55E-06	1.5	203.4
	2	8.186E-08	1.86E-09	8.40E-09	1.58E-08	4.47E-09	4.11E-10			
	5	2.046E-07	2.60E-09	1.08E-08	6.50E-08	1.79E-09	6.27E-10			
	8	3.274E-07	2.96E-09	2.28E-08	9.23E-08	5.63E-09	3.85E-10			
	11	4.502E-07	1.86E-09	3.57E-08	1.47E-07	8.67E-09	9.67E-11			
	14	5.73E-07	1.86E-09	4.23E-08	2.64E-07	6.78E-09	8.16E-11			
						<b>5.47E-09</b>	<b>3.20E-10</b>			
					Avg	2.57E-09	2.31E-10			
					±	E-09	10			

1 b	Inj #	[M] <sub>Total</sub>	[M] <sub>Monomer</sub>	[M] <sub>Dimer</sub>	[M] <sub>Tetramer</sub>	K <sub>D-T</sub>	K <sub>D-D</sub>	[Syr]	Δv	V
								6.43E-06	1.5	203.4
	2	9.484E-08	3.01E-09	9.00E-09	1.64E-08	4.94E-09	1.01E-09			
	5	2.371E-07	3.49E-09	1.78E-08	3.60E-08	8.79E-09	6.84E-10			
	8	3.794E-07	4.66E-09	2.04E-08	6.03E-08	6.92E-09	1.06E-09			
	11	5.216E-07	4.12E-09	2.65E-08	8.35E-08	8.44E-09	6.38E-10			
	14	6.639E-07	4.80E-09	2.94E-08	1.20E-07	7.24E-09	7.84E-10			
						<b>7.27E-09</b>	<b>8.36E-10</b>			
					Avg					

**E-09 10**

1.52 1.92E-

± E-09 10

1  
c

Inj #	[M] <sub>Total</sub>	[M] <sub>Monomer</sub>	[M] <sub>Dimer</sub>	[M] <sub>Tetramer</sub>	K <sub>D-T</sub>	K <sub>D-D</sub>
2	7.271E-08	2.90997E-09	9.04E-09	1.48E-08	5.52E-09	9.37E-10
5	1.818E-07	3.65909E-09	1.51E-08	3.70E-08	6.18E-09	8.85E-10
8	2.909E-07	4.11531E-09	1.97E-08	5.93E-08	6.53E-09	8.61E-10
11	3.999E-07	4.45634E-09	2.12E-08	8.15E-08	5.53E-09	9.35E-10
14	5.09E-07	4.73328E-09	2.34E-08	1.04E-07	5.27E-09	9.58E-10

[Syr]	Δv	V
4.93E-06	1.5	203.4

**5.81 9.15E-**

Avg **E-09 10**

5.28 4.07E-

± E-10 11

2  
a

Inj #	[M] <sub>Total</sub>	[M] <sub>Monomer</sub>	[M] <sub>Dimer</sub>	[M] <sub>Tetramer</sub>	K <sub>D-T</sub>	K <sub>D-D</sub>
2	4.848E-08	3.22397E-09	6.75E-09	7.57E-09	<b>6.01 E-09</b>	<b>1.54E-09</b>
6	1.454E-07	4.24298E-09	1.00E-08	2.27E-08	4.44E-09	1.79E-09
10	2.424E-07	4.82096E-09	1.13E-08	3.79E-08	3.37E-09	2.06E-09
14	3.393E-07	5.24404E-09	1.46E-08	5.30E-08	4.03E-09	1.88E-09
18	4.363E-07	5.58408E-09	1.86E-08	6.82E-08	5.09E-09	1.67E-09

[Syr]	Δv	V
4.93E-06	1	203.4

4.59 1.79E-

Avg E-09 09

1.01 1.98E-

± E-09 10

2  
b

Inj #	[M] <sub>Total</sub>	[M] <sub>Monomer</sub>	[M] <sub>Dimer</sub>	[M] <sub>Tetramer</sub>	K <sub>D-T</sub>	K <sub>D-D</sub>	
2	5.516E-08	3.22397E-09	6.75E-09	7.57E-09	<b>6.01E-09</b>	<b>1.54E-09</b>	
6	1.655E-07	4.24298E-09	1.00E-08	2.27E-08	4.44E-09	1.79E-09	
10	2.758E-07	4.82096E-09	1.13E-08	3.79E-08	3.37E-09	2.06E-09	
14	3.861E-07	5.24404E-09	1.46E-08	5.30E-08	4.03E-09	1.88E-09	
18	4.965E-07	5.58408E-09	1.86E-08	6.82E-08	5.09E-09	1.67E-09	
					Avg	4.59E-09	1.79E-09
					±	1.01E-09	1.98E-10

[Syr]	Δv	V
5.61E-06	1	203.4

2  
c

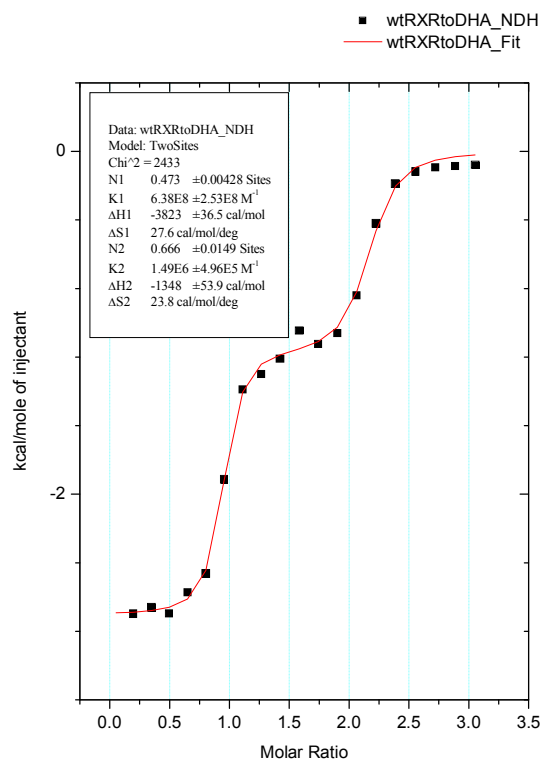
Inj #	[M] <sub>Total</sub>	[M] <sub>Monomer</sub>	[M] <sub>Dimer</sub>	[M] <sub>Tetramer</sub>	K <sub>D-T</sub>	K <sub>D-D</sub>	
2	7.758E-08	2.95773E-09	1.36E-08	1.21E-08	<b>1.52E-08</b>	<b>6.44E-10</b>	
6	2.327E-07	3.89259E-09	2.40E-08	3.64E-08	1.59E-08	6.30E-10	
10	3.879E-07	4.42284E-09	2.84E-08	6.06E-08	1.33E-08	6.88E-10	
14	5.431E-07	4.81098E-09	3.45E-08	8.49E-08	1.41E-08	6.70E-10	
18	6.982E-07	5.12294E-09	3.99E-08	1.09E-07	1.46E-08	6.58E-10	
					Avg	1.46E-08	6.58E-10
					±	9.92E-10	2.24E-11

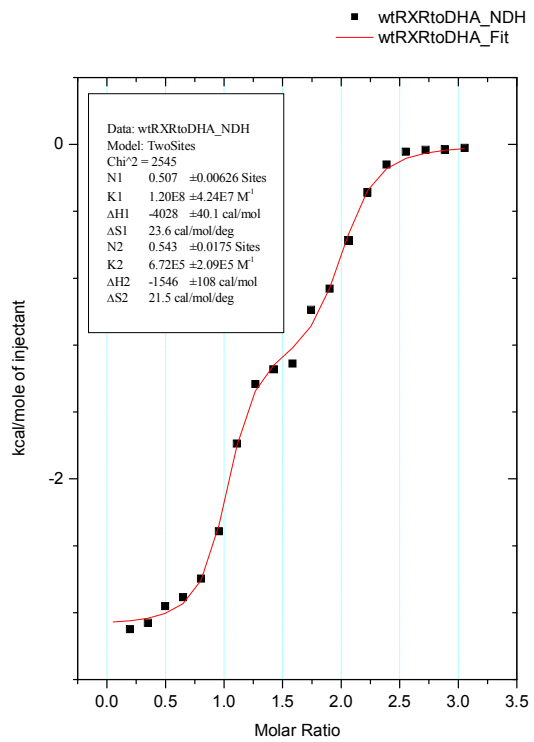
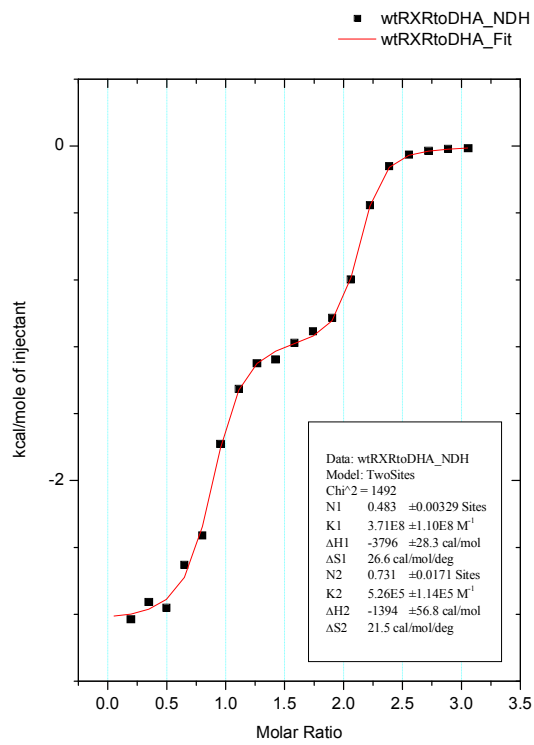
[Syr]	Δv	V
7.89E-06	1	203.4

## APPENDIX E

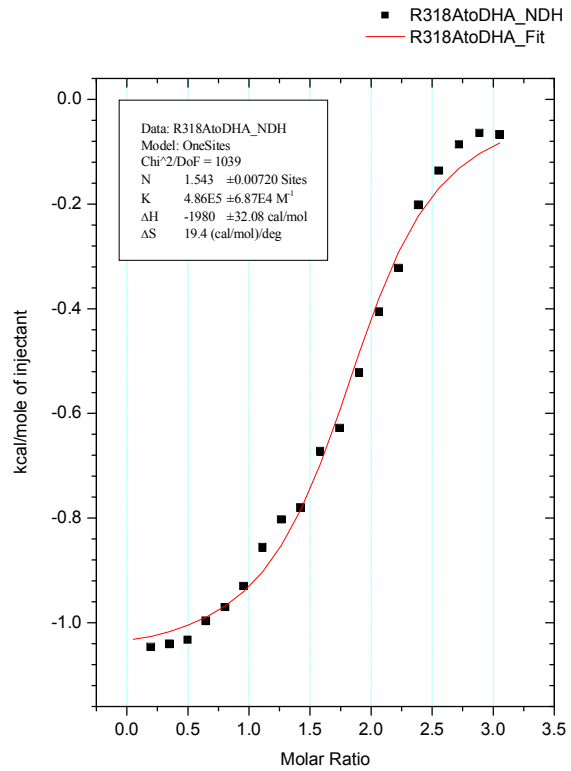
### ITC THERMOGRAMS

#### a) wtRXR with DHA

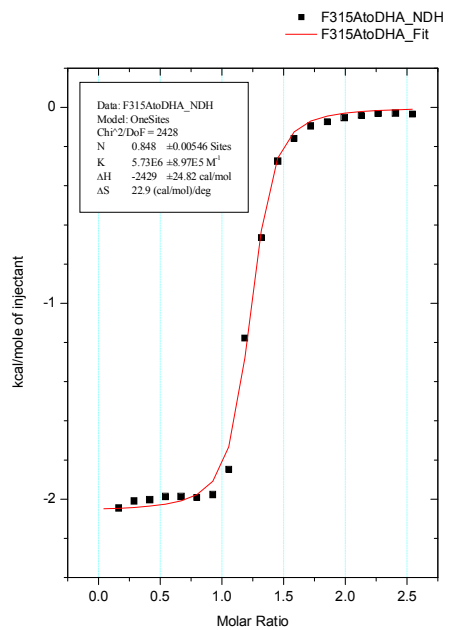
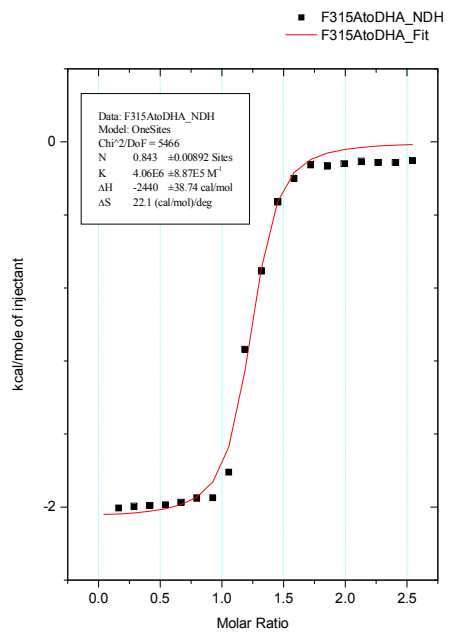




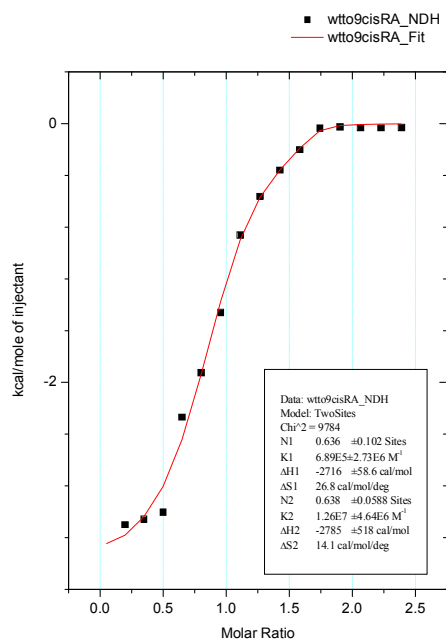
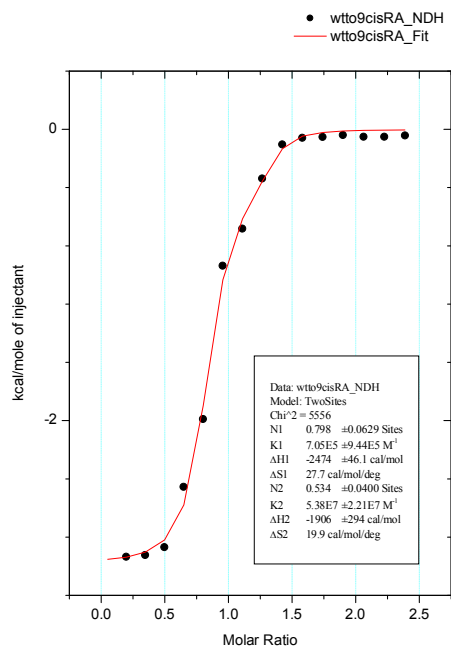
## b) R318A-RXR with DHA



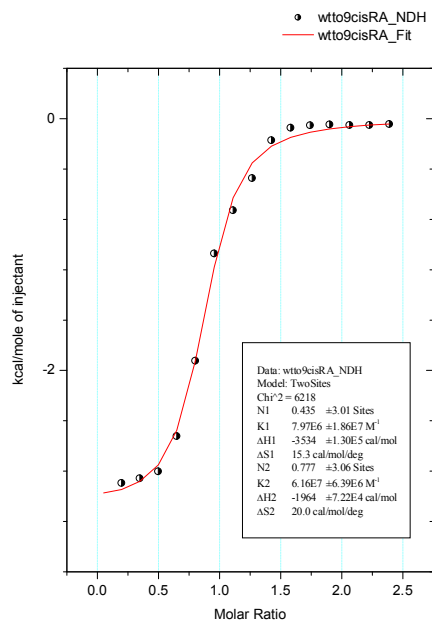
### c) F315A-RXR with DHA



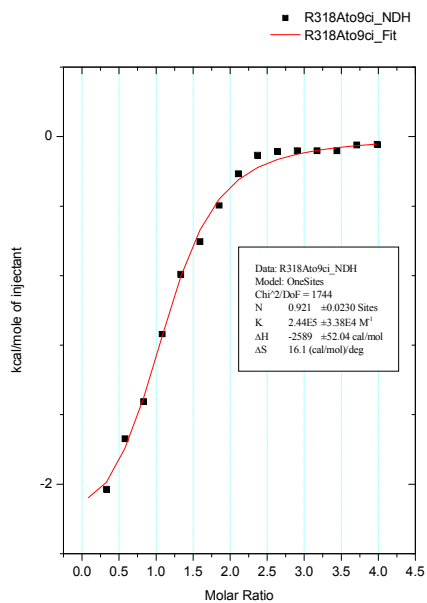
d) wtRXR with 9cisRA

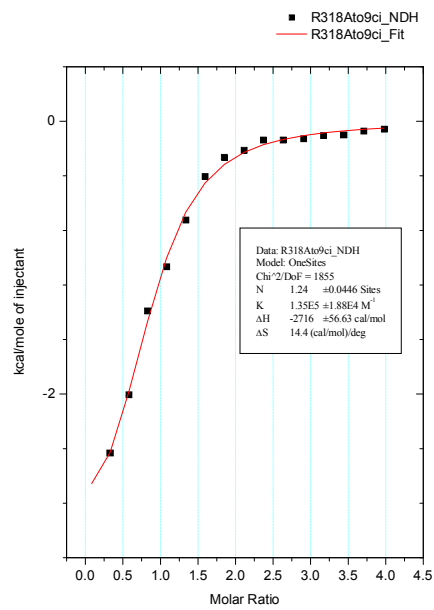
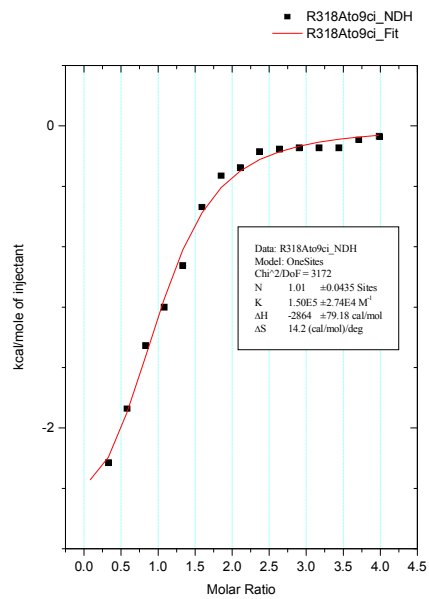




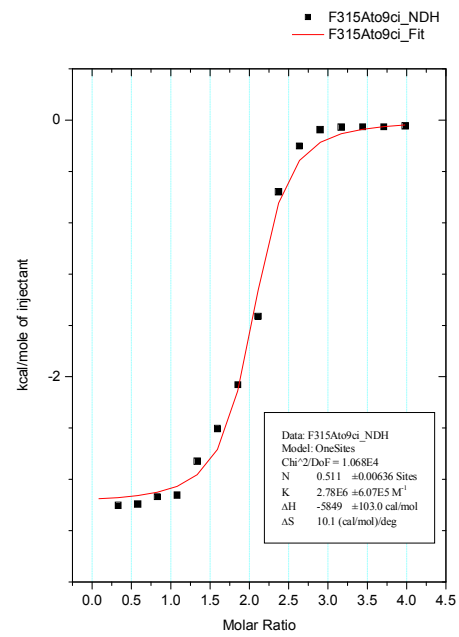
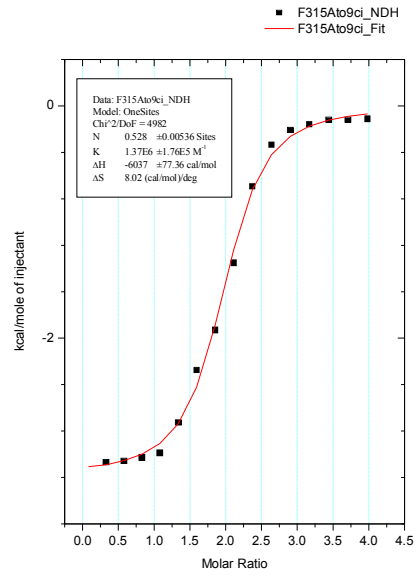


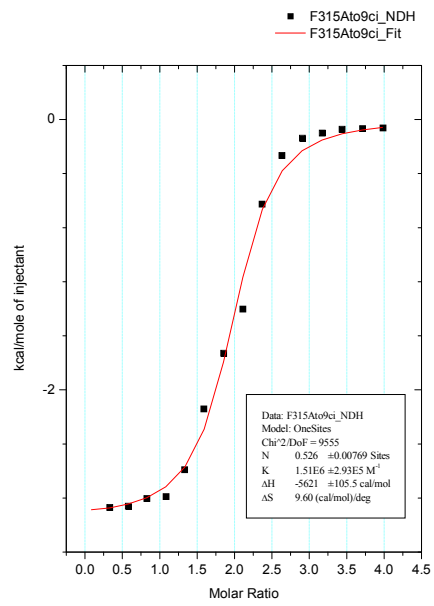
**e) R318A-RXR with 9cisRA**



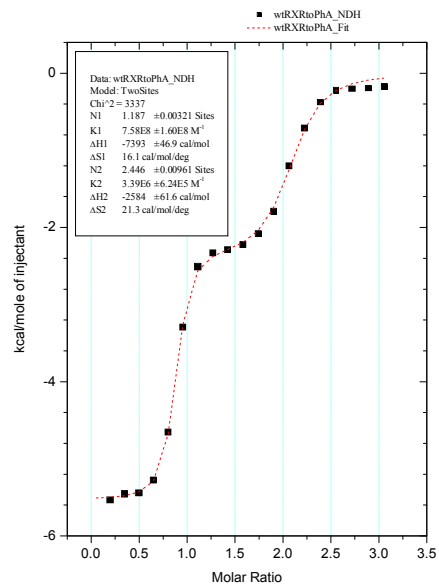


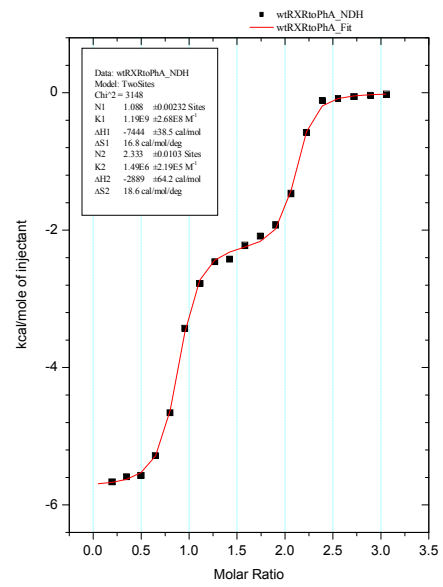
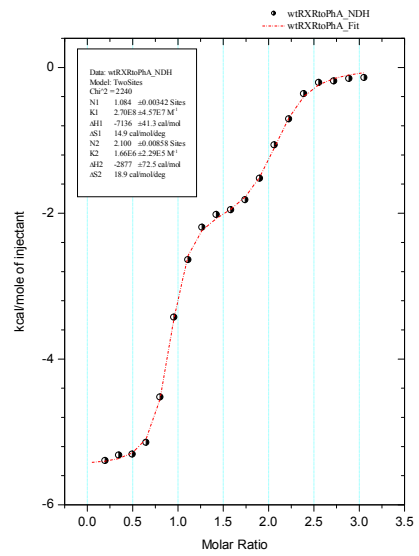
f) F315A-RXR with 9cisRA



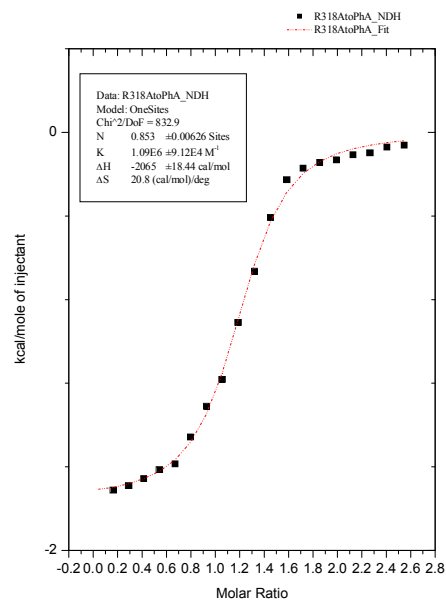
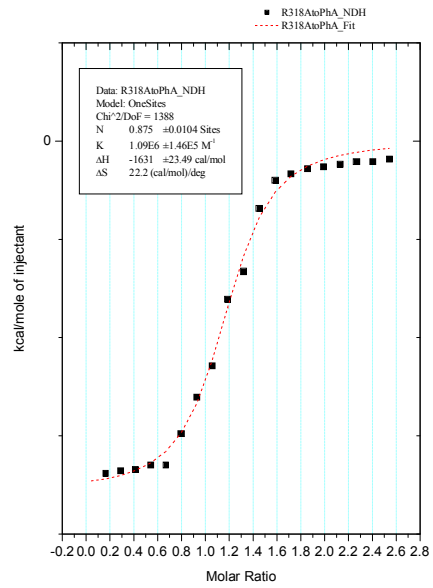


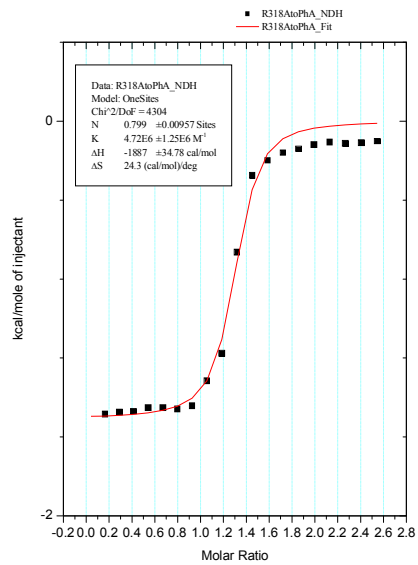
### g) wtRXR with Phytanic Acid



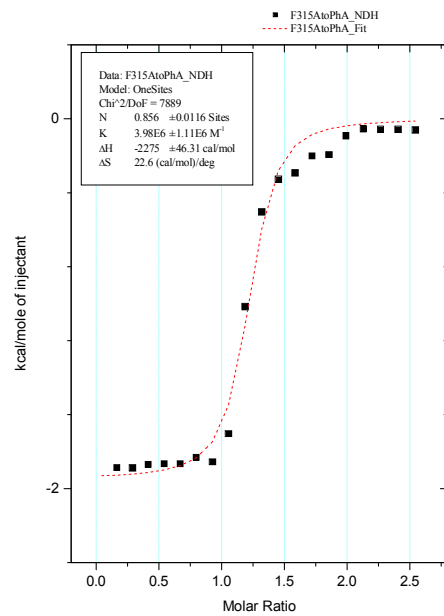


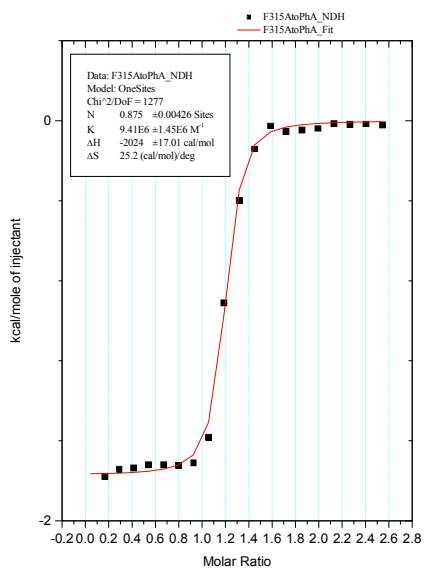
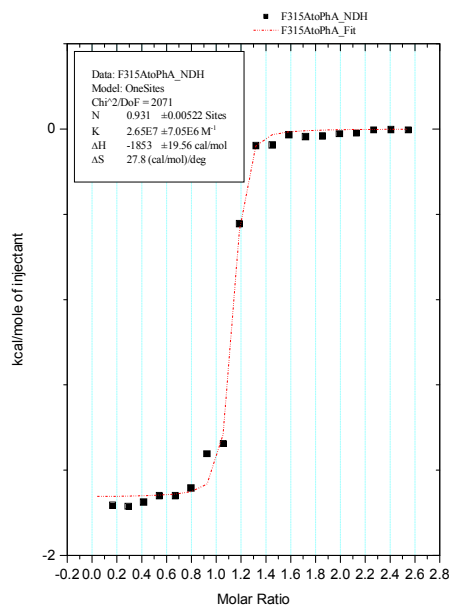
## h) R318A-RXR with Phytanic Acid





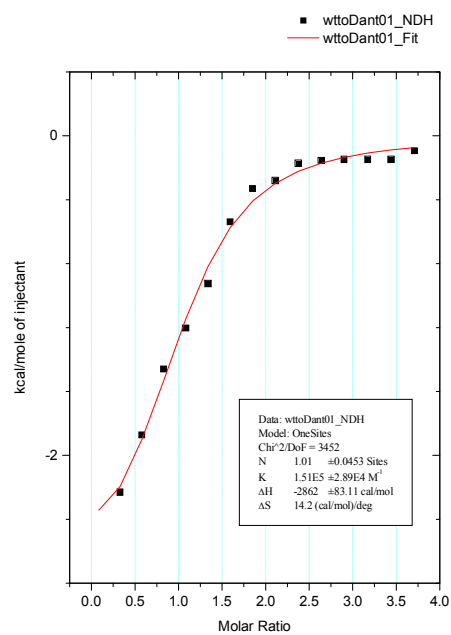
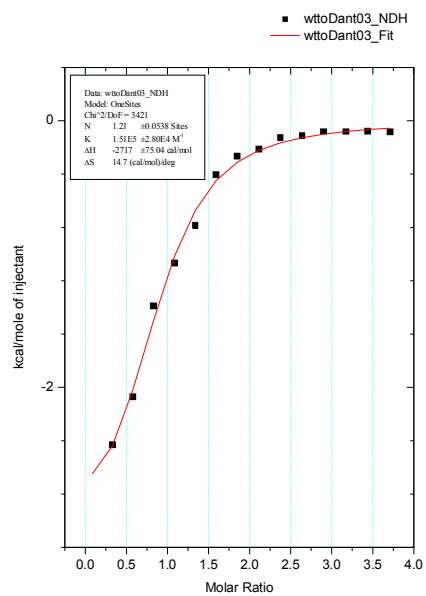
**i) F315A-RXR with Phytanic Acid**

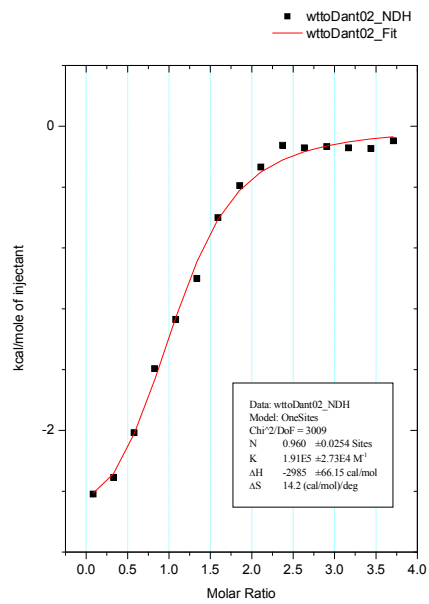




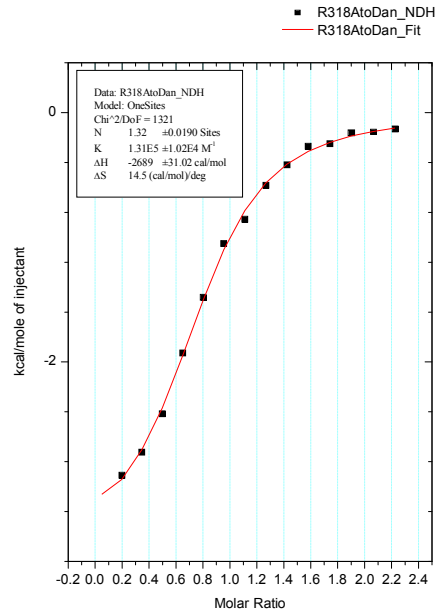


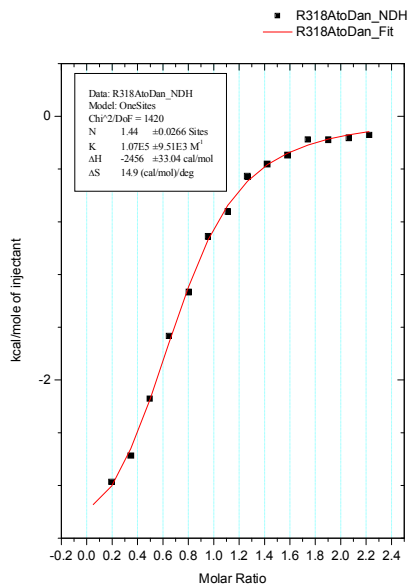
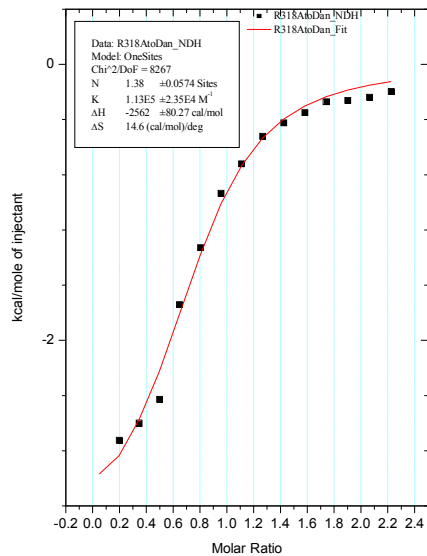
j) wtRXR with Dantron





**k) R318A-RXR with Dantron**





## j) F315A-RXR with Dantron

